UNIVERSITÀ DEGLI STUDI DI MILANO

Dipartimento di Scienze Cliniche e di Comunità

Scuola di Dottorato in Scienze Biomediche Cliniche e Sperimentali

Corso di Dottorato di Ricerca in Ematologia Sperimentale

Ciclo XXVII

IDENTIFICATION AND VALIDATION OF CRITICAL 1Q21 "ACHILLES HEEL" VULNERABILITES OF MULTIPLE MYELOMA

MARIANNA D'ANCA

Matricola R09533

Relatore: Prof. Antonino NERI

Correlatore: Prof.ssa Simona COLLA

Coordinatore : Chiar.mo Prof. Paolo CORRADINI

A. A. 2013/2014

TABLE OF CONTENTS

Summary

Summary

Multiple Myeloma (MM) is malignancy of terminally differentiated plasma cells characterized by a marked heterogeneity of genetic lesions and clinical course. Despite significant efforts towards the development of risk stratification strategies for patients with Multiple Myeloma (MM), we are still limited in our capacity to molecularly predict the natural history of these patients. Recent molecular analyses have illuminated many aspects of the pathogenesis of this heterogeneous disease, although there remains an elemental view of the compendium of genetic elements driving MM initiation and progression and how such genetic alterations functionally contribute to specific aspects of disease pathobiology, prognosis and treatment responses. Indeed, despite considerable progress in the management of MM patients, many studies have shown that some genetic alterations especially t(4;14) translocation, loss of the short arm of chromosome 17, loss of the long arm of chromosome 13 and amplification of chromosome 1q21 remain associated with a poor outcome and represent independent adverse predictors of shorter progression free survival (PFS) and overall survival (OS). The 1q21 amplicon is among the most frequent chromosomal aberrations in patients with MM (about 40% of *de novo* MM) and is considered a highly poor-risk genetic feature correlated with disease progression and drug resistance; it spans approximately a region of 10-15 Mb containing a large number of possible candidate genes. To date the relevant genes on 1q21 remain unclear and the absence of focal amplifications involving this region strongly suggests that more than a single candidate may represent the driver event responsible for poor outcome of this group of MM patients. Thus, the identification of critical 1q21 ‘Achilles heel’ vulnerabilities may yield a comprehensive catalog of the potential therapeutic targets for these high risk MM and provide a rationale for patient stratification. In an effort to accomplish this goal, we first identified a high-priority list of 78 copy number-driven 1q21 MM-relevant genes. Then, we have designed a high-throughput systematic shRNA screen approach *in vitro* to identify 1q21 genes whose loss of function results in selective death and/or growth inhibition of MM cells carrying the 1q21 amplification. After excluding shRNAs that display citotoxic activity regardless 1q21 amplification, we defined 1q21 “Achilles heel” vulnerabilities as shRNA target genes whose down-regulation decreases substantially the percentage of GFP-positive MM cells with 1q21 amplification over a time of 7 days based on a GFP-competion assay. This assay provided a list of candidate genes implicated in survival or proliferation of MM cells with 1q21 amplification; MCL1, UBAP2L, INTS3, LASS2, KRTCAP2, and ILF2. By targeting these six genes

we performed secondary validation experiments in JJN3 and H929 MM cell lines, carrying 4 copies of 1q21 amplicon. The results of this secondary validation confirmed that the down-regulation of these genes caused an important decrease of proliferation and increase of apoptosis as well as growth cycle arrest. Further GEP analysis and clinical outcome studies revealed that only UBAP2L and ILF2 showed a significant prognostic value but *in vivo* validation studies on NOD-SCID mice identified only ILF2 correlated with *in vivo* survival. So our studies focused to investigate the role of ILF2 in 1q21 amplified MM.

Nuclear Factor 45 (NF45) or ILF-2 is widely expressed in normal tissue with a predominant nuclear distribution. NF45/ILF2 associates with NF90/NF110 (ILF3) interacting with DNA and RNA. ILF2 and ILF3 contribute to gene regulation at different levels, transcription, splicing, nuclear exporting, but they are also involved in other important processes like mitotic control and DNA break repair.

Down-regulation of ILF2 in MM cells with 1q21 amplification resulted in multinucleated phenotypes and abnormal nuclear morphologies that were associated with a significant accumulation of γH2AX foci and DNA damage response activation, increased sensitivity to Melphalan, DNA damaging agent, and impaired activation of DNA repair pathways. Experiments of immunoprecipitation combined with mass spectometry showed that ILF2 interacts with numerous RNA binding proteins directly implicated in DNA repair or regulation of DNA damage response by modulating alternative splicing and stability of specific pre-mRNAs. Accordingly, RNA-sequencing analysis of ILF2-depleted MM cells, when compared to cells carrying scrambled shRNAs, identified specific changes in RNA splicing patterns before and after treatment with Melphalan.

Thus, our findings have raised a new tight correlation between 1q21 amplification and DNA damage response. We identified ILF2 as a key driver of this interaction, and our findings support the development of strategies designed to modulate ILF2 expression in patients with high-risk MM carrying 1q21 amplification providing personalized therapies for patients who do not benefit from recent treatment improvements.

Introduction

Multiple Myeloma

Multiple Myeloma (MM) is a genetically complex disease that is becoming more common in today's ageing population. MM is a Plasma-Cell (PC) malignancy characterized by the accumulation of terminally differentiated clonal PCs in the Bone Marrow (BM), the production of a monoclonal immunoglobulin (Ig) detectable in serum and/or urine and the presence of lytic bone lesions [{4}]. In the Western countries MM accounts for approximately 2% of all cancer-related deaths, and in the USA constitute approximately 20% of all hematological malignancies [{1}]. The incidence of MM increases with age and the patient median age with MM is 65 years, but 3% of them are younger than 40 years [{2}]. MM remain an incurable disease and the median length of survival after diagnosis is three to five years. Although some evidence for genetic predisposition, genetic background and environmental role remain to be clarified [{3}].

Clinical features and pathogenesis of multiple myeloma

Multiple myeloma is caused by the growth of a malignant plasma cell clone in the bone marrow, leading to severe clinical symptoms that include hypercalcaemia (occurring in 25% of patients), renal dysfunction (50%), anemia (70%), and bone disease (frequently referred to by the acronym CRAB) which represent evidence of end organ failure [{4}]. The presence of one or more of these four markers related to the underlying plasma cell disorder is required for the diagnosis of the disease.

The initiation and progression of myeloma at the present it is believed developing via multistep process where an initiating hit is required to immortalize a Myeloma-Propagating Cell (MPC) that is destined to acquire additional genetic hits over time [{5}] (Figure 1).

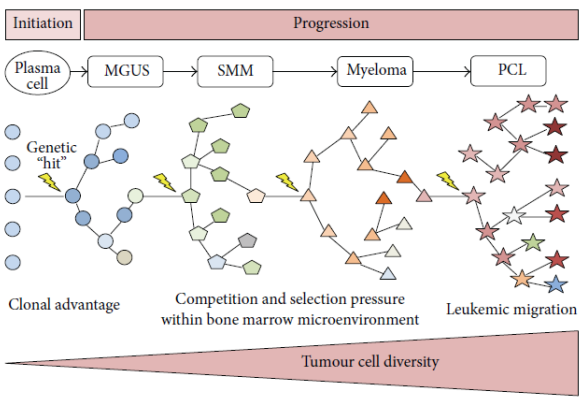

Figure 1: Initiation and progression of Myeloma.

In many instances MM is preceded by a pre-malignant tumor called Monoclonal Gammopathy of Undetermined Significance (MGUS), which is the most common lymphoid tumor in humans, occurring in approximately 3% of individuals over the age of 50[{6}]. The transition from MGUS to Plasma Cell Leukemia (PCL) has been traditionally represented as a linear pathway but more likely the pathway to myeloma is through branching pathways. A post-Germinal Centre (GC) B cell receives a genetic hit which immortalizes the cell and starts the transition to the indolent phase of MGUS. More genetic hits which confer a survival advantage and are acquired over time, allow to MGUS clones to pass through the other disease phases of SMM (Smoldering Multiple Myeloma), myeloma, and PCL. Clonal evolution develops through branching pathways whereby numerous ecosystems composed of multiple subclones exist at each disease phase, as represented by the differing shapes. At the end of this process, proliferative clones no longer become confined to the bone marrow and expand rapidly as a leukemic phase. At each disease phase, the precursor clones are present only at a low level as they have been outcompeted by more advantageous clones. This multistep process permits myeloma to have various recognizable clinical phases, distinguished by biological parameters, along its development (**Table 1**).

MGUS (Monoclonal Gammopathy of Undetermined Significance)

- M-protein in serum <30 g/L
- BM clonal PC <10% and low level of PC infiltration in the trephine biopsy (if done)
- No evidence of other B cell proliferative disorders
- No MM-related organ or tissue impairment (no end organ damage, including bone lesions)

SMM (Smoldering Multiple Myeloma)

- M-protein in serum $\geq$30 g/L **and/or** BM clonal PC $\geq$10%
- No evidence of other B cell proliferative disorders
- No MM-related organ or tissue impairment (no end organ damage) or symptoms

MM (Multiple Myeloma)

- M-protein in serum and/or urine (M protein in most cases is >30g/L (>25g/L sometimes used for IgA) and >1g/24hr of urine light chain but some patients with symptomatic MM have lower than these)
- BM clonal PC or plasmacytoma (Monoclonal PC usually exceed 10% of nucleated cells in the BM but no minimal level is designated because about 5% of patients with symptomatic MM have <10% BM PC)
- No evidence of other B-cell proliferative disorders
- Related organ or tissue impairment (no end organ damage, including bone lesions)

Plasmacytoma

Solitary plasmacytoma of the bone

- No M-protein in the serum and/or urine (a small M-component may sometimes be present)
- Single area of bone destruction due to clonal PC
- BM not consistent with MM
- Normal skeletal survey (and magnetic resonance imaging (MRI) of spine and pelvis if done)
- No MM-related organ or tissue impairment (no end organ damage other than solitary bone lesions)

Extramedullary plasmacytoma

- No M-protein in serum and/or urine (a small M-component may sometimes be present)

- Extramedullary tumour of clonal PC
- Normal BM
- Normal skeletal survey
- No MM-related organ or tissue impairment (no end organ damage other than solitary bone lesions)

Non-secretory MM
- No M-protein in serum and/or urine with immunofixation
- BM clonal plasmacytosis ≥10% or plasmacytoma
- Related organ or tissue impairment (end organ damage, including bone lesions)

Plasma cell leukemia
- Absolute PC count in peripheral blood ≥2.0 x 109/l
- Peripheral blood differential white cell count with >20% PC

Amyloidosis
- Presence of an amyloid-related systemic syndrome
- Positive amyloid staining by Congo red in any tissue (e.g. fat aspirate, BM, organ biopsy)
- Evidence that amyloid is light chain-related established by direct examination of the amyloid
- Presence of a monoclonal PC disorder

Myeloma related organ or tissue impairment (CRAB)
Hypercalcemia (serum calcium >11.5mg/dl) (**C**), renal insufficiency (serum creatinine >177µmol/L) (**R**), anemia (hemoglobin <10g/dl) (**A**); bone lesions: lytic lesions or osteoporosis with compression fractures (MRI may clarify) (**B**). Other: symptomatic hyperviscosity, amyloidosis, recurrent bacterial infections (> two episodes in 12 months) [{136}].

Table 1: Diagnostic criteria for PC neoplasms [{135}].

MGUS is an indolent, asymptomatic, premalignancy phase characterized by a small clonal population of plasma cells within the bone marrow of <10% [{6}]. MGUS has a prevalence of >5% in adults aged over 70 and a progression risk to myeloma quantified at 1% per year [{7,8}]. The next asymptomatic phase is SMM that is distinguished from MGUS by a greater intramedullary tumour cell content of >10% and an average risk of progression to myeloma of 10% per year for the first five years [{9}]. Next, myeloma itself is recognized; whereby malignant clones cause clinically relevant end-organ damage including the features of CRAB. There are no unequivocal genetic or phenotypic markers that distinguish MGUS from MM tumour cells, so that it is not possible to predict if and when an MGUS tumour will progress to MM. Also, it remains unclear to what extent intrinsic genetic or epigenetic changes in MGUS tumour cell versus extrinsic changes in non-tumour cells affect progression. The final phase is PCL, an aggressive disease end-point characterized by the existence of extramedullary clones and rapid progression to death (Figure 2). Some of these extramedullary multiple myelomas can establish immortalized cell lines *in vitro*.

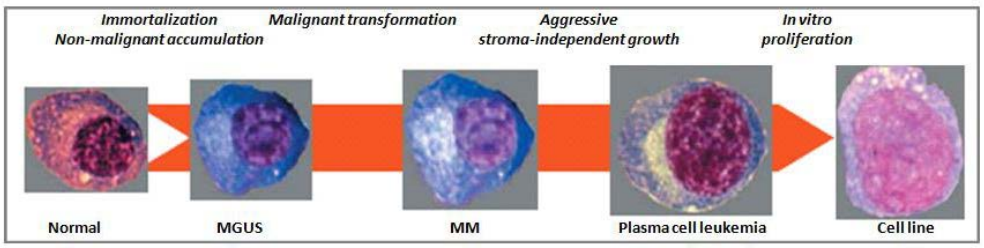

Figure 2: Progression through the different stages of Multiple Myeloma.

Multiple myeloma cells are the transformed counterparts of post-germinal center bone marrow plasmablasts/plasma cells arising from malignant transformation of plasma cell or their precursors {9}.

Initially, multiple myeloma is confined to the bone marrow (intramedullary), but with time the tumour can acquire the ability to grow in extramedullary locations (such as blood, pleural fluid and skin). The strong association with the stromal cells of the BM makes MM cells phenotypically similar to long-lived PCs but also the immunophenotype looks like that of normal long-lived bone marrow PC ($CD19^{-}CD20^{-}CD45^{-}CD138^{+}$){1}. Despite to them MM is able to proliferate at very low rate, usually with no more than a few percent of cycling cells until advanced stages of MM {10}.

Deregulation of myeloma cellular pathways and processes

Several signaling pathways deregulated in MM play crucial roles in promoting growth, survival, adhesion, migration, immortalization, angiogenesis, and drug resistance {82}.

Other cellular processes such as DNA repair, RNA editing, protein homeostasis, and cell differentiation may also contribute towards myeloma genesis through aberrant functioning.

NF-kB pathway

The importance of NF-kB pathway in MM is supported by the evidence that at least 50% of cases and 20/44 HMCLs show the NF-kB pathway constitutively active {67;68}. Moreover also several studies suggest the relevance of NF-kB signaling in MM, by the nuclear presence of NF-kB in MM cells and the sensitivity of some MM cell lines to NF-kB inhibition {83,84}. Interestingly, not only in plasma cells but also in surrounding bone marrow stromal cells the pathway of NF-kB can be upregulated following production of IL6, BAFF, or APRIL, known growth factors for and activators of NF-kB in MM {83}.

In myeloma cell lines and patient samples different mechanisms may deregulate NF-kB pathway both inactivating pathway suppressors due to deletions and/or mutations and hyperactivating NF-kB target gene expression including NF-kB-inducing kinase (NIK), TRAF3, CYLD, BIRC2/BIRC3, CD40, NFKB1, or NFKB2 {67}. Moreover whole genome sequencing (WGS) and whole exome sequencing studies suggested a broader role of NF-kB signaling by discover of 10 novel point mutations and 4 structural rearrangements affecting 11 members of the NF-kB pathway {60}. Nevertheless, although the importance of deregulated NF-kB pathway in myeloma pathogenesis is attested, the prognostic impact for many of the implicated genes are yet to be fully investigated.

The Mitogen Activated Protein Kinase (MAPK) pathway

The MAPK pathway, involved in cell differentiation, proliferation, and survival, may be stimulated through a variety of inflammatory cytokines, including TNF-α, IL-6, and IGF-1, which alternately activate the downstream kinase cascades RAS, RAF, MEK, and MAPK influencing gene expression. N-RAS and K-RAS are the two dominant oncogenes in the MAPK pathway frequently mutated in myeloma. The prevalence of activating N- or K-RAS mutations is nearly 20–35% in the newly diagnosed MM tumors {85} and 45% in HMCLs {86}. It should be noticed that the prognostic impact between the two different forms of RAS could not be equal because some studies have shown that N-*RAS* mutations were more common that K-RAS mutations {85}. This represents an important finding if genetic lesions are used to define risk. Patients with *RAS* mutation have more aggressive disease features and significantly shorter overall survival and progression free survival despite similar response to therapy.

Interestingly, the incidence of RAS mutation in MGUS is less than 5% compared to MM {60}, this evidence is consistent with the hypothesis that RAS mutation might be an important progression event from MGUS to MM {87}. Thus because RAS mutation represents the single most frequently mutated gene in myeloma, therapeutic inhibitors in its pathway are searching.

The JAK-STAT pathway

Nearly 50% of myeloma samples and a quote of surrounding BM stromal cells have JAK-STAT pathway constitutively activated {88,89}. JAK-STAT activation seems occurring mainly through autocrine and paracrine stimulation of IL-6, an important cytokine in myeloma genesis that regulates growth and survival of MM cells {90}.

Indeed the activation of this pathway leads to hyperactivity of the transcription factor STAT3, which results in elevated expression of the antiapoptotic protein Bcl-xL/BCL-2 {91}. On the other side the STAT3 knockdown or IL-6 receptor blockade may cause apoptosis in some HMCLs but only in absence of the BM microenvironment {92}. This finding indicates that IL-6R/STAT3 signaling is dispensable within the context of the BM microenvironment, which might stimulate IL-6–independent pathways that protect MM cells from apoptosis {92}.

The Phosphatidylinositol-3 Kinase (PI3K) Pathway

It has been suggested that the dysregulation of PI3K pathway may be significant in myeloma cells growth and survival as a number of cytokines including IL-6 and IGF-1 can be activate it via phosphorylation of the serine-threonine-specific kinase AKT. The latter is an indicative marker of PI3K activity and its phosphorylation is detected in approximately 50% of cases. Afterwards downstream targets of AKT including mTOR and GSK-3β can be activated and influence many processes including cell proliferation and apoptosis resistance {93}. Despite of MAPK pathway, the PI3K pathway is not frequently mutated in myeloma {94}. Anyway the pathway can potentially be therapeutically targeted at different points such as inhibition of phosphorylation/activation of AKT and inhibition of PI3K itself {95}.

Translocation and cyclin D (TC) classification

Cyclin D genes are expressed at low levels in quiescent cells, while in response to growth factors they are transcriptionally up-regulated and expressed in all proliferating cells. Despite the very low proliferative activity observed in PC from MGUS/SMM and MM patients, the level of CCND1, CCND2 or CCND3 mRNA in all these tumors was found to be relatively high compared with the level of CCND2 mRNA expression in healthy proliferating PC {96} making the dysregulation of a cyclin D gene a unifying oncogenic event. This up-regulation of cyclin D genes is caused by either IgH translocations or other, unknown mechanisms.

Gene expression profiling can detect the expression levels of CCND1, CCND2, and CCND3 and simultaneously identify spiked expression of genes deregulated by primary IgH translocations. Supervised analysis of gene expression profiles provided the basis for a molecular classification of MM: the translocation and cyclin D (TC) classification (**Table 2**).

Group	Primary Translocation	Gene at Breakpoint	D-Cyclin	Ploidy	Proliferation Index	Bone disease (% MRI Pos)	Frequency (%)	Prognosis
6p21	*6p21*	*CCND3*	D3	NH	Average	100	3	? Good
11q13	*11q13*	*CCND1*	D1	D, NH	Average	94	16	Good
D1	None	None	D1	H	Low	86	34	Good
D1+D	None	None	D1 and D2	H	High	100	6	? Poor
D2	None	None	D2	H, NH	Average	67	17	?
None	None	None	None	NH	Average	100	2	? Good
4p16	*4p16*	*FGFR3/MMSET*	D2	NH O H	Average	57	15	Poor
maf	*16q23*	*c-maf*	D2	NH	High	55	5	Poor
	20q11	*mafB*					2	

Abbreviations: MRI, magnetic resonance imaging; pos, positive; D, diploid; H, hyperdiploid; NH, nonhyperdiploid.

Table 2: Translocation and Cyclin D (TC) groups.

Thus Bergsagel et al. developed the translocation/cyclin D (TC) classification (Figure 3), subdividing myeloma patients into 8 subgroups based on the presence of genes (in)directly dysregulated by translocations and cyclin D overexpression: (**1**) 4p16 tumors (15%) expressing high levels of CCND2 and MMSET (and in most cases FGFR3) as a result of the translocation t(4;14); (**2**) MAF tumors (7%) expressing the highest levels of CCND2 and showing high levels of either c-MAF or MAFB, consistent with the possibility that both MAF transcription factors up-regulate the expression of CCND2; (**3**) 11q13 (16%) and (**4**) 6p21 (3%) tumors expressing high levels of either CCND1 or CCND3 as a result of an IgH translocation; (**5**) D1 tumors (34%) ectopically expressing low to moderate levels of CCND1 despite the absence of a t(11;14) translocation; (**6**) D1+D2 (6%) expressing both CCND1 and CCND2. (**7**) D2 tumors (17%) were a mixture of tumors expressing CCND2; (**8**) none (1%) expressed no D-type cyclins. The TC classification did not clearly identify patients with HRD MM. HRD tumors were mainly found in the D1 and D1+D2 groups. D1 and D2 HRD MM appeared to have a higher incidence of proliferative disease compared to D1 HRD MM characterized by a low proliferative index. However, no differences in survival were noted between the two groups [{96}].

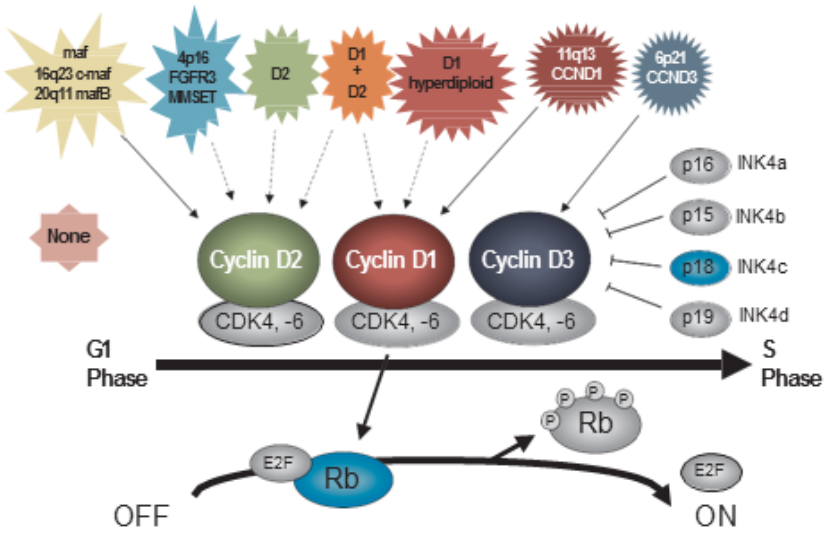

Figure 3: Dysregulation of one of the three cyclin D can be a consequence of *Ig* translocations (solid arrow) or by an unknown mechanism (dashed arrow)[137].

Genetic architecture and disease progression

At the cytogenetic level MM genome is complex and more reminiscent of epithelial cancers than of more simple leukemia. Many of the genetic lesions that lead to MM have been defined, and can be categorized as inherited variation, traslocations, copy number abnormalities, mutations, methylation, and miRNA abnormalities.

Chromosomal translocations

Multiple Myeloma is essentially a complex genetic disease characterized by marked karyotype instability and almost all cases of MM are cytogenetically abnormal [11].

Like a normal long-lived plasma cell, a myeloma cell undergoes three developmentally regulated changes in the DNA structure of the immunoglobulin heavy chain and light chain (IgH and IgL) loci, including V(D)J recombination of its IgH and IgL genes, somatic hypermutation of the IgH and IgL variable regions, and productive IgH switch recombination to another IgH isotype [12]. As result of having undergone these processes, the Ig genes in plasma cells (PCs) from myeloma patients are characterized by heavily mutated V_H regions with no intraclonal variation and carry isotype-switched IgH genes (IgG or IgA) [13], and also chromosomal translocations targeting the immunoglobulin H (IgH) locus (at 14q32.3), and less frequently the IgL locus (2p12, or 22q11) [14,15,16]. These aberrant rearrangements juxtapose oncogenes into the proximity of the powerful IGH enhancers, driving abnormal expression of the translocated oncogenes. This enables the cells to survive and proliferate, resulting in immortalization of the malignant cell clone. The translocations of the IGH at 14q32 are

associated to the non hyperdiploid myeloma subtypes distinguished from the hyperdiploid myeloma subtypes which are characterized by trisomies of certain odd numbered chromosomes, 3, 5, 7, 9, 11, 15, 19, and 21 with a low prevalence of chromosomal translocations (Figure 4).

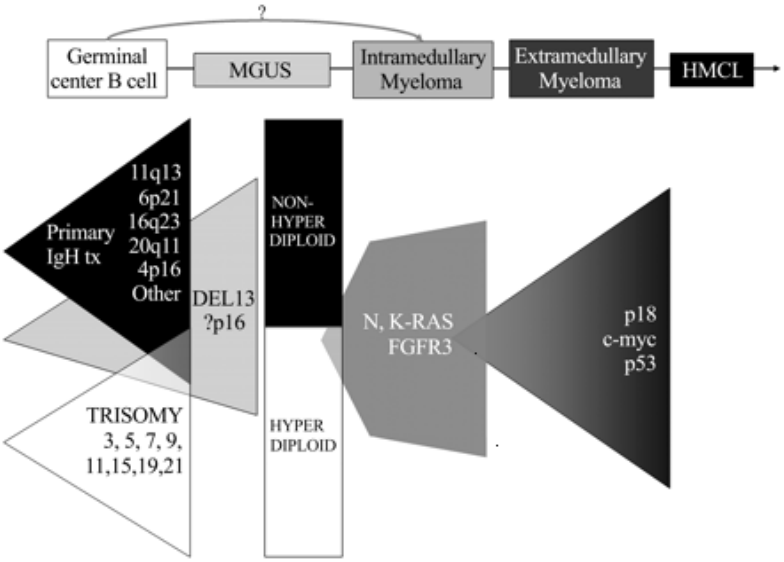

Figure 4: In MM two distinct pathways have been recognized: a nonhyperdiploid (nonHRD) (black triangle) that usually includes one of seven recurrent IgH translocations as an early event and a hyperdiploid (HRD) pathway (white triangle) which is associated with multiple trisomies of odd numbered chromosomes.

Hyperdiploid and non hyperdiploid changes appear to represent early or even initiating mutagenic events that are followed by secondary aberrations including copy number abnormalities, additional translocations, mutations, and epigenetic modifications which lead to plasma cell immortalization and disease progression.

Primary translocation

Karyotypic instability begins from the earliest phase of MM and increases with stage disease. The IgH translocations can be observed in approximately 50% of patients with MGUS or SMM, 55%-70% of intramedullary MM, 85% in primary PLC and > 90% of myeloma cell lines [1; 17,18,19]. The translocations involving the IgH locus at 14q32 have five recurrent partner chromosomes: 11q13 (CCND1, the most common), 4p16.3 (MMSET/FGFR3), 6p21 (CCND3), 16q23 (c-*MAF*), and 20q11 (MAFB)[20] and they are identified in approximately 40% of MM tumors representing markers for distinct myeloma subtypes with important prognostic implications.

The breakpoints of these translocations mostly occur within or near switch regions, and sometimes within or near VDJ sequences, suggesting that they could be mediated by

mistakes in IgH switch recombination or somatic hypermutation. There is no evidence that IgH switch recombination or somatic hypermutation mechanisms are active in normal PC or PC tumors, so it is presumed that these translocations usually represent primary, perhaps initiating, oncogenic events as normal B cells pass through germinal centers.

MMSET/FGFR3 translocation group

The t(4;14), found in 15% of myeloma cases using FISH analysis, has been associated with an adverse prognosis in a variety of clinical settings [21,22]. Pathologically the juxtaposition next to the IGH 3' enhancers, leads to the overexpression of two genes, Fibroblast Growth Factor Receptor 3 gene (FGFR3) on der(14) and the Multiple Myeloma SET domain gene (MMSET) on der(4)[22]. The up-regulation of FGFR3 implies the ectopic expression of the FGFR3 tyrosine kinase receptor, an aberration with an unclear role in myeloma genesis. Gene expression profiling and RT-PCR analysis have shown that only 70% of the MM with t(4;14) display a simultaneous overexpression of MMSET and FGFR3. As approximately 30% of t(4;14) tumors are imbalanced due to lack of FGFR3 expression following the loss of the der(14), the pathogenic role of FGFR3 is somewhat in doubt although in some cases der(14) is present and other mechanisms account for the loss of FGFR3 expression [19;23]. Furthermore, in these 30% lacking FGFR3 expression, the adverse prognosis of t(4; 14) remains[21], lending support for the role of the second gene MMSET. MMSET, encoding a chromatin-remodelling factor with histone methyltransferase (HMT), is overexpressed in all MM harboring the t(4; 14) which represents the only known mechanism that dysregulates MMSET[24]. Sometimes rare tumors with t(4;14) can acquire kinase-activating mutations of the dysregulated FGFR3 during tumor progression, and there is evidence that the survival and proliferation of these tumours is dependent on the mutated FGFR3[25,26]. Although epigenetic regulation and a role in DNA repair have been suggested, like FGFR3, the exact role of MMSET in the pathogenesis of MM is still unclear [27,28].

Cyclin D translocation group

The t(6;14) is a translocation present in only 2% of myeloma patients and acts upregulating directly the CCND3 gene via juxtaposition to the IGH 3' enhancers [29] while t(11;14) is more common, observed in approximately 17% of myeloma patients

and also directly upregulates a cyclin D gene, CCND1[30]. Gene expression profiling studies have shown that the overexpression of CCND3 and CCND1 results in a clustering of downstream gene expression suggesting that activation of these two genes results in the dysregulation of common downstream transcriptional programs [24]. Unlike t(4;14), the overall prognostic impact of these two translocations is neutral although t(11;14) patients show considerable heterogeneity and in some cases the translocation may manifest with an aggressive phenotype such as PCL[31].

MAF translocation group

The t(14;16) and t(14;20) both result in increased expression of a MAF family oncogene and combined are identified in 5–10% of presenting myeloma cases. In detail, t(14;16) results in overexpression of c-MAF, a transcription factor which upregulates a several genes like CCND2 and other genes (ITGB7, ARK5) that appear to affect the phenotype of the tumor cells, and its potential interactions with the bone-marrow microenvironment [32,33].

The t(14;16) is commonly associated with a poor prognosis [22;34], although this concept has recently questioned by retrospective multivariate analysis on 1003 newly diagnosed myeloma patients which showed t(14;16) not to be prognostic [35], t(14;20) is the rarest translocation involving the IGH locus and results in upregulation of the MAFB gene. It seems that also MAFB could deregulated the same downstream targets of cMAF because MAFB overexpression showed a similar gene expression profile to that seen with cMAF [24]. Notably, t(14;20) is associated with a poor prognosis when present in myeloma but correlates to long-term stable disease when found in MGUS and SMM [36]. This observation suggests that MAF deregulation alone is not responsible for the adverse outcomes but that additional genetic events are required.

Secondary Translocations

As myeloma tumors become more proliferative at later stage of disease, secondary translocations occur but in contrast to primary translocations, they represent class-switch recombination independent events that do not involve B cell specific processes. The most frequent secondary translocation is t(8;14) observed in only 3% of MM [37,38]. The gene typically deregulated is MYC and its overexpression is linked directly to late disease stages and indirectly to a poor prognosis via a strong correlation to high levels of an established indicator of a poor prognosis, the serum β2-microglobulin

(Sβ2M) [38,40]. The frequency of MYC overexpression from secondary translocations reflects its role as a progression event, as it is absent o rare in MGUS but seen in 15% of myelomas, 50% of advanced disease and 90% of HMCL (Human MM Cell Line) [38;41]. These secondary events often include unbalanced and complex translocations and insertions that can involve three chromosomes, sometimes with associated amplification, duplication, inversion, or deletion. Thus MYC rearrangements are thought to represent a very late progression event that occurs when MM tumors are becoming less stromal-cell-dependent and/or more proliferative [1].

Other IgH translocation partners have been identified in approximately 20% of MGUS and MM tumors [17,18,19]. These other partners, who are poorly characterized, appear to be mostly non-recurrent or rare. These translocations seem to share the structural complexity and lack of IgH switch region involvement observed for MYC translocations, suggesting that they usually represent secondary translocations, which can occur at any time during tumor progression, including MGUS. Translocations involving an Igλ locus occur in about 10% of MGUS tumors, and approximately 20% of advanced MM tumors or HMCLs [1;17]. Translocations involving an Igκ locus are rare, occurring in only a few percent of MM tumors. Nearly half of IgL translocations in advanced MM tumors or HMCL target a MYC gene. Significantly, although all HMCLs analyzed have either an IgH or IgL translocation, whereas approximately 30% of MM tumors and 45% of MGUS tumors do not have either an IgH or IgL translocation. Surprisingly, however, two independent Ig translocations have been found in 5% of MGUS tumors, 25% of advanced MM tumors, and 58% of HMCL, consistent with an accumulation of secondary Ig translocations during tumor progression [17].

Copy number variations in Myeloma

Copy number variations result from gains and losses of DNA and are common events in myeloma. These gains and losses can be both focal or of an entire chromosome/chromosome arm. In general, losses of DNA contribute to malignancy through loss of tumour suppressor genes, whereas gains are pathogenic through oncogene overexpression/activation.

Aneuploidy

Approximately 50% of myeloma cases are hyperdiploidy ((HD) 48-75 chromosomes) involving trisomies of the odd numbered chromosomes 3, 5, 7, 9, 11, 15, 19, and 21, but only infrequently (<10%) have one of the recurrent IgH translocations [{42}]. More common in aged patients and associated with a high incidence of bone disease; hyperdiploidy confers a relatively favorable prognosis in the majority of cases [{43}]. The remaining cases, non-hyperdiploidy (NHD) subtypes, can be hypodiploid (up to 44/45 chromosomes), pseudodiploid (44/45 to 46/47) or near tetraploid (more than 74), and usually (~70%) show one of the recurrent IgH translocations[{44}].

In contrast to the selective event of recurrent IgH translocations in NHD tumors, other genetic events (17p loss or p53 mutations, RAS mutations, secondary Ig translocations, MYC translocations) often occur with a similar prevalence in HD and NHD tumors, while loss of chromosome 13 occurs in 72% of NHD tumors but only 37% of HD tumors, which is explained partially by the increased prevalence of t(4;14) and t(14;16) in NHD tumors[{45}].

For tumors that are hyperdiploid but have one of the recurrent translocations, most often a t(4;14), we do not know whether hyperdiploidy occurred before or after the translocation since the underlying mechanism to generate hyperdiploidy is unknown. However, one can make the hypothesis, based on what is suggested to occur in hyperdiploid acute lymphoblastic leukemia, of a single catastrophic mitosis results in the gain of whole chromosomes rather than their serial accumulation over time [{46}]. Not only the underlying mechanism but also the consequence of hyperdiploidy towards myeloma genesis is poorly understood. Anyway recent GEP studies have demonstrated that hyperdiploid myeloma is characterized by overexpression of genes involved in protein biosynthesis, specifically ribosomal protein genes representing end-points in important signaling pathways of myeloma biology as MYC, NF-κB, and MAPK. This finding raises the possibility that one consequence of this protein biosynthesis profile in hyperdiploid myeloma is deregulation and overproduction of oncogenic proteins [{47}].

Loss of Chromosome 13/13q14

Approximately 50% of myeloma cases [{19; 48, 49,50}] and 40-50% of MGUS [{18;48}] present deletion of chromosome 13 suggesting that often this is an early event in the pathogenesis. In around 85% of cases, deletion of chromosome 13 occurs like a whole-chromosome monosomy [{51,52}] or loss of the q arm, whereas various interstitial

deletions have been observed in the remaining 15% of cases, keeping a level of gene function[51]. Nevertheless the identification of key genes contributing to myeloma pathogenesis is a challenging, molecular studies have shown that the tumour suppressor gene RB1 is significantly underexpressed in del(13/13q) resulting in inferior negative cell cycle regulation[53]. The prognostic impact of del(13/13q) is also a challenging because it is frequently associated with other high-risk lesions, like t(4;14) in approximately 90% of cases[54]. When del(13/13q) is detected via conventional cytogenetics there is a link to poor survival[55,56], whereas when detected via FISH, and in the absence of coexisting high-risk lesions, the linkage with survival is lost[57;31]. This finding suggests that the historical link between del(13/13q) and a poor prognosis come from its association with high-risk lesions.

Loss of 1p

Around 30% of myeloma patients show whole arm deletion or interstitial deletions of the 1p chromosome. This deletion is associated with a poor prognosis [53;58,59] but molecular genetic studies have revealed that two regions of 1p, 1p12, and 1p32.3 are mainly important in myeloma pathogenesis when deleted. In detail 1p12 region contains the candidate tumour suppressor gene FAM46C whose function is unknown, although its expression seems correlated to factors involved in protein translation [60]. FAM46C seems an important gene in myeloma as it has been shown to be frequently mutated and also independently correlated to a poor prognosis [53;58;60,61]. 1p32.3 contains the two target genes, FAF1 and CDKN2C. The latter is a cyclin-dependent kinase 4 inhibitor involved in negative regulation of the cell cycle, whereas FAF1 through the Fas pathway encodes a protein involved in initiation and/or enhancement of apoptosis. Homozygous deletion of 1p32.3 is associated with prognosis based on the treatment to whom patients are subjected, for those who received ASCT the prognosis is poor, for the other ones its prognostic impact is neutral [58]. Although some evidences place CDKN2C like the influential gene lost through homozygous 1p32.3 deletion [58;62], the significance of FAF1 related to CDKN2C remains to elucidate as most of deletions lost both genes that lie in close proximity.

Loss of 17p

Most of chromosome 17 deletions involve the whole p arm in approximately 10% of new myeloma cases but the frequency of mutations appears to increase with disease

stage becoming approximately of 30% in PCL[19;63]. It is believed that the relevant gene deregulated in del(17p) being the tumour suppressor gene TP53 but there is not definitive evidence that the critical chromosome 17p loss is TP53. However there are some findings that could be able to support this hypothesis. In GEP studies myeloma samples with monoallelic 17p deletions express significantly less TP53 compared to non-deleted samples [53]. Furthermore, patients that do not have the del(17p) the rate of TP53 mutation is <1%, whereas in those with del(17p) this rises to 25–37% [64].

The TP53 gene maps to 17p13 and is known that it is a transcriptional regulator of cell cycle arrest, DNA repair, and apoptosis in response to DNA damage. In myeloma, del(17p) represents the most important molecular prognostic indicator as it linked to an aggressive disease phenotype, a greater degree of extramedullary disease, and short survival[19;31;65]. Furthermore, 65% of HMCLs show TP53 deficiency, further suggesting its relevant role in extramedullary disease. Most of PCL cases have abnormalities in TP53 gene so it is assumed that PCL might be largely a consequence of TP53 dysfunction [63], but it should be noticed that there is no direct biological evidence supporting this hypothesis, and the genetic consequences of the deletion need to be further clarified.

Other Chromosomal Losses

Many other chromosomal losses are observed in myeloma, and like in the deletions of 1p, 13/13q, and 17p, they are "driver" lesions that contribute to myeloma pathogenesis because the regions involved contain tumor suppressor genes. An important deletion, observed in the 7% of myeloma cases, concerns chromosome 11q where the tumour suppressor genes BIRC2 and BIRC3 are located. More common is the del(14q), the site of the tumor suppressor gene TRAF3, founded in 38% of cases [53]. Another common deletion is the 16q, seen in the 35% if myeloma cases, that harbor the tumor suppressor genes CYLD and WWOX[53]. All of these genes, except WWOX implicated in apoptosis [65], are involved in the nuclear factor-kB (NF-kB) pathway, indicating that up-regulation of NF-kB signaling is important in myeloma pathogenesis [53;67,68].

Del(6q) and del(8p), seen in 33% and 19-24% of cases, are other two common chromosomal arm deletions [53;69,70] but the significance of del(6q) towards survival is still not clear. Instead del(8p) acts as an independently poor prognostic factor for both progression free survival (PFS) and overall survival (OS) [69]. Furthermore, the tumor necrosis factor-related apoptosis-inducing ligand receptor genes (TRAIL-R1 and

TRAIL-R2) located on 8p, show a down-regulation due to del(8p) [71]. In *vitro*, TRAIL was shown to play pivotal roles in inducing apoptosis in HMCLs and in immune surveillance. Thus, mutation of TRAILR1 and TRAIL-R2 may contribute to the loss of its apoptotic function and provides a growth advantage to cancer cells [70].

Gain of 1q

Comparative genomic hybridization (CGH) and fluorescence in situ hybridization (FISH) have revealed chromosomal gains of 1q, which may occur as iso-chromosomes, duplications, or jumping translocations [110]. Nearly 35-40% of myeloma cases show the gain of the chromosome 1q arm (+1q) representing one of the most frequent chromosomal aberrations observed in MM [53;61]. These gains are concentrated substantially in those tumours that have a t(4;14) or t(14;16), or an high proliferation rate [72,73]. The 1q21 amplification is related to an advanced phenotype of MM and associated with disease progression [74]. Indeed the incidence of Amp1q21 increases with stage disease; 0% in MGUS, 45% in SMM, 43% in newly diagnosed MM, 72% in relapsed MM, and 91% in human myeloma cell lines [73]. It is considered a highly-poor risk genetic feature correlated with a poor prognosis in newly diagnosed MM and a shortened post-relapse survival and may be central to progression of plasma cell dyscrasias [73]. There was no notable improvement in survival of patients with 1q21 gains when treated with chemotherapy incorporating bortezomib, implying that 1q21 gains might be linked to bortezomib resistance and drug resistance [75,76].

1q21 region: copy number aberrations and target candidate genes in multiple myeloma

Chromosome 1, one of the largest chromosomes, has 3141 genes and many overlapping coding sequences. This is the reason why it represents a likely candidate for genetic events that lead to malignant transformation[{110}]. The gain of the 1q21 region is a cytogenetic marker for high-risk multiple myeloma, occurs frequently, about 40% of cases, and is often found in proliferative relapsed and/or refractory disease [{75;77;97}]. Many studies have shown that those genetic alterations represent independent adverse predictors of shorter progression free survival (PFS) and overall survival (OS) [{39; 108}].
As reported in the study of Hanamura and colleagues, the frequency of Amp1q21 increases with disease progression and at relapse was significantly higher than in newly diagnosed MM (Figure 5).

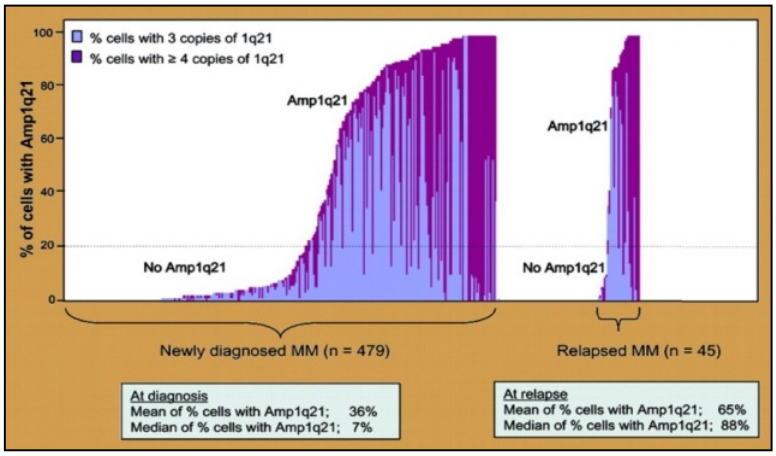

Figure 5: Proportion of cells with Amp1q21 at diagnosis and relapse.

Many data also demonstrated that the gain of 1q21 is also different in the different stage of the disease (**Table 3**).

MGUS	
Total	0/14 (0)
Progression, +	0/1 (0)
Progression, –	0/13 (0)
SMM	
Total	14/31 (45)
Progression, +	10/12 (83)
Progression, –	4/19 (21)
MM	
At diagnosis	205/479 (43)
At relapse	33/45 (72)

Table 3: 1q21 amplification in different stages of disease

A German group found that the clinical course of patients with more than three copies of 1q21 was characterized by a remarkable short PFS and OS, whereas exactly three copies of 1q21 were associated with only a marginal effect on outcome {81}. However the Arkansas group reported that patients with more than three copies of 1q21 at diagnosis had similar 5-year event-free survival (EFS) and OS compared with those with three copies of 1q21 {73} (Figure 6). The clinical translation of this finding is still under discussion, since patients with amplifications of 1q21 can't benefit from alternative therapeutic strategies such as thalidomide {110}.

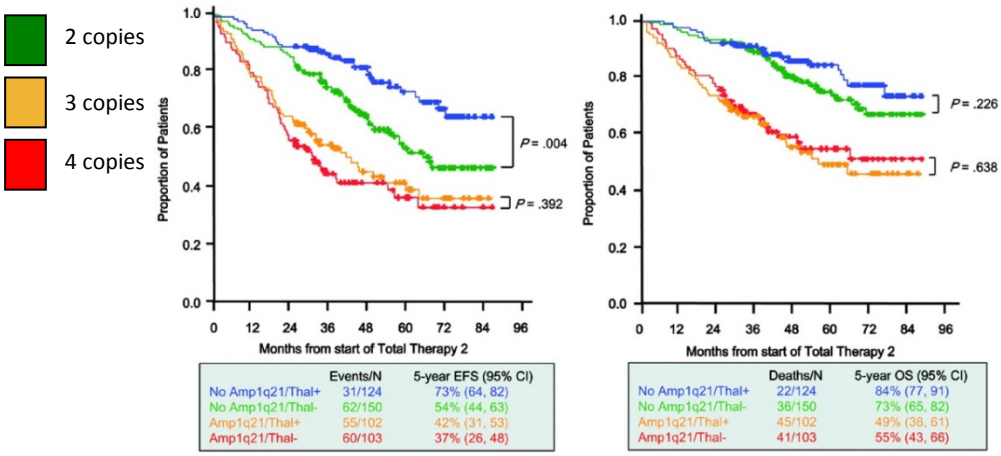

Figure 6: A Kaplan-Meier analysis of EFS (left) and OS (right) is displayed in relation to no Amp1q21 (up to 2 copies of 1q21, n = 124) or Amp1q21 (3 or more copies of 1q21, n = 102) in patients treated with a regimen containing thalidomide and in relation to no Amp1q21 (n = 150) or Amp1q21 (n = 103) in patients treated with a regimen without thalidomide. Thal+ indicates patients treated with thalidomide; Thal-, patients treated without thalidomide.

The cellular and molecular mechanisms of 1q21 amplifications are not well understood and to date the relevant genes on 1q are not fully explored. Both aCGH and GEP studies have identified one region of proximal 1q with a marked enrichment of genes showing a gain and/or amplification which spans approximately a region of 10-15 Mb corresponding to a 1q21-23 amplicon in MM {77}. In detail GEP studies found that cases with 1q21 gains showed significantly altered expression of genes involved in Unfolded Protein Response (UPR), including upregulation of chaperone gene CLN3, UBAP2L, and UBE2Q1, proteasome degradation gene PSMD4 and CASP4 gene involved in UPR-induced apoptosis {78}. Integrating GEP and DNA variation copy number variation data, several independent studies revealed that numerous 1q21 genes are copy number sensitive in MM {77;79}. Because UPR induced apoptosis plays an

important role in the sensitivity of malignant cells to bortezomib, these studies strongly suggest that bortezomib resistance gene overexpression is associated with 1q21 chromosome gains. Recently, Shaughnessy et al. reported that hyperexpression of proteasome PSMD4 (Proteasome 26S subunit, non-ATPase-4) residing on chromosome 1q21 was a novel high-risk feature in myeloma treated with Total Therapy 3 [80]. The same group identified a strong prognostic association with an increased level of CKS1B (CDC28 protein kinase regulatory subunit 1B), located on 1q21 chromosome, suggesting that it may contribute to disease progression [111-112]. Fonseca and colleagues, assessing the 1q21 gain by FISH and the increased expression of CKS1B by GEP on two separated cohorts of patients respectively (n=159, n=67), showed that neither 1q21 gain nor increased CKS1B expression are independent prognostic factors in MM and also 1q21 gain has a more significant impact on the survival than CKS1B overexpression but importantly they didn't find evidence for a copy number-driven expression of CKS1B [72]. Another candidate gene located on the 1q21 chromosome is MUC1 (Mucin1). Several studies reported that MUC1 is detected on the majority of MM cell lines, MM patient cells and MM B cells [113-114] and its levels are related to MM disease burden. It is aberrantly expressed in MM cells and there is one early study that supports a model in which the inhibition of MUC1 had a synergistic effect with Bortezomib to kill Bortezomib resistant cells[115]. Also MCL1 (Myeloid cell leukemia 1), a BCL2 family member, maps to 1q21 chromosome and it is considered a critical survival factor for MM [104]. Zhang et al. showed a rapid activation of apoptosis if only MCL-1 was inhibited, even with continuous expression of other antiapoptotic proteins. This gene may be an attractive therapeutic target [104]. BCL9, located on chromosome 1q, is frequently a target of amplification and is associated with aberrant expression [77; 109]. In the work of Mani and colleagues BCL9 is overexpressed in a subset of MM cells and it plays fundamental roles in tumor progression but they didn't observe a significant relationship between BCL9 DNA copy number and mRNA expression in MM patients. Thus, additional mechanisms are involved in the up-regulation of BCL9 [109]. The last interesting gene emerged as a candidate target is PDKZ1. The over-expression of this gene is reported in a variety of carcinomas [116] but its role in the tumorigenesis is still unknown. This gene in primary MM tumor is frequently amplified and Inoue and coworkers suggested that PDZK1 is one of potential targets for chromosomal gain of 1q21 region, likely associated with drug resistance phenotype in MM [117]. In summary, although these findings suggest that

1q21 locus harbors target genes associated with myelomagenesis, the essential target genes for chromosomal gain involving 1q21 region in MM remains obscure. Furthermore, the absence of focal amplifications involving this region strongly suggests that more than a single candidate may represent the driver event responsible for poor outcome of this group of MM patients. Thus, the identification of critical 1q21 "Achilles heel" vulnerabilities may yield a comprehensive catalog of the potential therapeutic targets for these high-risk MM patients and provide a rationale for patient stratification.

Aim of the study

The 1q21 amplification is among the most frequent chromosomal aberrations in patients with Multiple Myeloma (MM) and is considered a highly poor-risk genetic feature correlated with disease progression and drug resistance. So the identification of critical 1q21 'Achilles heel' vulnerabilities may yield a comprehensive catalog of the potential therapeutic targets and provide a rationale for patient stratification. To accomplish these goals we have designed first a high-throughput systematic shRNA screen approach *in vitro* to identify 1q21 genes whose loss of function results in MM cell death and/or growth inhibition. This assay provided a list of candidate genes implicated in survival or proliferation of MM cells with 1q21 amplification; MCL1, UBAP2L, INTS3, LASS2, KRTCAP2, and ILF2. By targeting these six genes with specific shRNAs, we performed secondary validation experiments in human myeloma cell lines harboring four copies of 1q21 amplicon. The results confirmed that the down-regulation of these genes caused an important decrease of proliferation and increase of apoptosis as well as growth cycle arrest. Then *in vivo* validation studies identified only ILF2 correlated with *in vivo* survival. This result was confirmed also by GEP analysis and clinical outcome studies. Further analyses have focused to investigate the role of ILF2 in 1q21 amplified MM. My project has been performed with the tight cooperation of Dr. Simona Colla and her group at the Leukemia Department of MD Anderson Cancer Center in Houston.

Materials and Methods

Cell lines

All the cell lines used in this study (OCI-MY5, JJN3, H929, 293T) were purchased from American Type Culture Collection (ATCC). HMCLs and 293T were grown respectively in RPMI or DMEM medium supplemented L-glutamine (Gibco®, Life Technologies), 10% fetal bovine serum (Gibco®), and 100U/ml penicillin/100 mg/ml streptomycin (Gibco®). All the cells were maintained at 37°C in a 5% CO_2 atmosphere.

Xenograft models

Mice were sacrificed when the tumor was more than 20 mm in diameter following the IACUC (Institutional Animal Care and Use Committee) protocol; for subcutaneous tumors the maximum allowable size is 20 mm in diameter for a mouse. If the animal is host to more than one tumor, this size is the maximum allowable size for all tumors combined.

Cell survival and proliferation/apoptosis assays

Cell viability was evaluated every 24 hours by Trypan Blue exclusion assay. This evaluation was coupled to static assessment by FACS-based cell cycle analysis for quantitative S phase measurements via Propidium Iodide (PI; Sigma-Aldrich®) incorporation. Furthermore 4',6- diamino-2-phenylindole (DAPI; Sigma-Aldrich®) and Annexin V (Affimetrix®) staining were adopted for the secondary validation screening after 4 days from infection, according to the manufacturer's instructions, for measurement of cell viability and apoptosis.

High-throughput screening in 96 well format

To overcome major barriers of transgenesis in multiple myeloma (MM) cells, we have developed a high-throughput screening strategy in 96 format based on a single hairpin GFP-competition assay in which the differential survival of transduced cells is assayed by changes in the percentage of GFP positive cells over a time of 7 days. Using this format we are currently able to obtain an efficiency of infection of up to 70% (range 40-70%) in established MM cell lines: OCI-MY5 and JJN3. Briefly 1q21 shRNA pGipz lentiviral library composed of 532 shRNAs targeting 78 genes (Dharmacon®) was used to transfect in 96 wells the 293T cell lines. Each single shRNA is located in a different well but in each plate 3 wells were designed for the not silencing negative control and 3 for the positive

control. After the high-throughput lentiviral production JJN3 cell line carrying the 1q21 amplification and OCI-MY5 cell line without the 1q21 amplification were infected separately by lentiviral shRNAs, targeting each of 78 copy number-driven amplified 1q21 genes previously identified by our oncogenomic studies. The screen was done in triplicate using a single-shRNA-per-96 well format (an average of 5 sequence-verified GFP-based shRNAs for each gene will be used). A GFP competitive assay was adopted to identify the only genes whose knockdown decreased the percentage of GFP positive cells (4 days after lentiviral infection) over a time of 7 days. The GFP percentage in each plate was detected using the Canto II Analyzer (BD Biosciences®).

Western Blotting

We performed Western blotting analysis according to standard protocols. Briefly cells were lysed in the Mammalian Cell Extraction Buffer (BioVision®) supplemented with 1,4-Dithiothreitol 1M (BioVision®), Protease Inhibitor Cocktail 500x (BioVision®) and Phosphatase Inhibitor Cocktail 20x (Roche®). Whole cell lysates (30µg per cell line) were separated using the 4-12% NuPAGE® Bis-Tris Precast Gels (Novex®, Life Technologies) with MOPS SDS running buffer (Thermo-Fisher Scientific®) and electro-transferred on Nitrocellulose membranes (Bio-Rad®) for 1 hour at 100V on ice. The membranes were immunoblotted with primary antibodies overnight and then incubated with horseradish peroxidase-conjugated secondary antibodies (Pierce®,Thermo-Fisher Scientific) for 1 hour. Immuno-positive bands were visualized by enhanced chemiluminescence (Pierce®, Thermo-Fisher Scientific) according to the manufacturer's instructions. The primary antibodies anti-γ-H2AX, anti-pATM, anti-pCHK2, anti-Cleaved Caspase 3, anti-β-Actin, anti-pNBS1, anti-Cleaved PARP and anti-YB1 came from Cell Signaling Technologies® (CST), anti-vinculin was purchased from Sigma-Aldrich®; the anti-RNA binding protein and the heterogeneous nuclear ribonuclearproteins antibodies came from Santa Cruz Technologies®; anti-ILF2 and anti-LamininA were purchased from Millipore® and Abcam® respectively. Lastly anti-ILF3 p110 and anti-ILF3 p90 primary antibodies came from Origene® and Abcam® respectively.

Compound treatment and time course experiments

Melphalan powder (Sigma-Aldrich®) was resuspended in Dimethyl sulfoxide (DMSO) and added in JJN3 growing medium at 25μM concentration. Cells were harvested at the indicated time point to be processed for Western blot analysis with the procedure specified above. ImageJ software (W.Rasband, NIH) was used to quantify Western blot signals.

Nuclear-Cytosol fractionation

Nuclear/Cytosol fractionation was performed as specified in the protocol enclosed in the Kit (Biovision®) and 10μg of nuclear and 30μg of cytoplasmic proteins were loaded.

Immunoprecipitation

Protein A-agarose (Roche®) was washed twice with 0.1M Phosphate Buffer (Boston BioProducts®), before 2 hours incubation with 20μg of target or unspecific antibody (Rabbit/Mouse IgG; Santa Cruz®) at 4°C in gentle agitation. For the crosslinking, beads were washed three times with 50mg/ml Bovine Serum Albumine (BSA; Sigma-Aldrich®) in 1xPBS before the 30 minutes of incubation with 1:1 ratio pH8.2, 0.2M Triethanolamine (Sigma-Aldrich®)/Dimethyl pimelimidate dihydro-chloride (Sigma-Aldrich®) at room temperature. This incubation was repeated two times with a wash in pH8.2, 0.2M Triethanolamine in between. Then beads were incubated in pH8.2, 50mM Ethanolamine (Sigma-Aldrich®) for 10 minutes at room temperature for two times with a wash in 1xPBS in between. Elution of not specific proteins was carry out with two incubations of 5 minutes with pH 3.00 1M Glycine (Thermo Fisher Scientific®). Finally, beads were washed four times with NP-40 Lysis buffer (Boston BioProducts®) supplemented with Phosphatase/Protease inhibitor (Roche®). Cell lysate was resuspended in NP-40 Lysis buffer and incubated in ice for 15 minutes. After one cycle of sonication at 20% of the power (S400 Misonix Instrument®) 1mg of proteins was used in every single immunoprecipitation. Protein sample and beads were incubated for 3 hours at 4°C in gentle agitation and then washed three times with NP-40 Lysis buffer. Proteins were then eluted by adding NuPage (Life Technologies®) in a 1:1 ratio for 2 minutes at room temperature and then for 5 minutes at 70°C. Before loading gel 2-Mercaptoethanol (Bio-Rad®) at 2.5% of the final concentration was added to each sample.

Mass spectrometry analysis

Not Silencing (NS), ILF2#1, ILF2#2 JJN3 cells treated or untreated with 25µM Melphalan for 10 hours, were immunoprecipitate for ILF2 protein how described above. 4%-12% Agarose gel (Invitrogen®) was used to separate protein and, after that, stained with Silver Stain Kit following the vendor protocol (Pierce®). Silver-stained gel pieces were washed, destained (using the reagents in the Pierce kit) and digested in-gel with 200ng modified trypsin (sequencing grade, Promega®) in 50mM ammonium bicarbonate for 18 hours at 37ºC. Resulting peptides were extracted and analyzed by LC-MS/MS on an Orbitrap-Elite mass spectrometer (Thermo Scientific®). Proteins were identified by searching of the fragment spectra against the SwissProt (EBI) protein database using Mascot (v 2.3, Matrix Science, London, UK). Typical search settings were: mass tolerances, 10 ppm precursor, and 0.8d fragments; variable modifications, methionine sulfoxide, pyro-glutamate formation; trypsin, up to 2 missed cleavages. As suitable candidates only peptides that were not appeared in the control lane were considered.

RNA-Seq sequencing and analysis

An initial sequence-level quality assessment was performed using FastQC (version 0.10.1, Simon Andrews). The RNA-seq reads were then mapped to the human (GRCh37) reference genome using Tophat2[{98}], allowing a maximum of two mismatches per 75bp sequencing end. The NCBI RefSeq gene model and HTSeq software (version 0.5.4p2, Simon Anders) were used to quantify the gene-level expression levels. The differential analyses for gene/isoform expression were analyzed with DESeq2[{99}]while differential splicing was analyzed with rMATS[{100}].

Immunofluorescence

MM cells were resuspended in 1xPBS, spotted on immunofluorescence slides (Thermo Scientific®), fixed for 30 minutes in 4% paraformaldehyde (Sigma-Aldrich®), permeabilized in 0.2% Triton X-100 (Promega®) for 5 minutes and blocked in 5% BSA for 1 hour. Then, cells were stained with anti phospho-γH2AX (Millipore®), or phospho-ATM (CST®) primary antibodies. Alexa Fluor-555 and Alexa Fluor-488 (Life Technologies®) were used as secondary antibodies. Nuclei were stained with DAPI (Sigma-Aldrich®).

Indirect immunofluorescence microscopy

Cells were spotted on Superfrost Microscope Slides (Fisher Scientific®) via cytospin (1200 RPM for 7 minutes) and fixed with 4% paraformaldehyde (Sigma-Aldrich®) 10 minutes at 4°C. After 0.2% TritonX-100 (Promega®) permeabilization, cells were blocked in a 1xPBS with 5% BSA and 5% Goat Serum (Sigma-Aldrich®) 1 hour at room temperature. Cells were then stained with primary antibodies, diluted in the blocking solution, for 1 hour at room temperature and counterstained with secondary antibodies 45 minutes at room temperature. Cell nuclei were stained with DAPI before mounting coverslip with ProLong Gold Antifade mounting solution (Life Technologies®). Images were collected using a wide field and confocal microscope (Nikon Instruments Inc.®) and processed using ImageJ software (W.Rasband, NIH).

Binucleation and Nuclear aberrant structures evaluation

Cell nuclei were stained using DAPI (Sigma-Aldrich®) and wide field microscope transmission light permitted us to highlight cell cytoplasm. The analysis of abnormal nuclear morphologies (ANMs) was performed on binucleated cells following the criteria described by Fenech [{101}]. A nucleoplasmic bridge was considered to be the narrow/wide chromatin segment connecting two cell nuclei, micronuclei were morphologically identical to, but smaller than the cell nucleus, and round or oval protrusions of the nuclear membrane, connected to the cell nucleus were classified as bud [{101}].

Results

High-throughput screening for candidate genes

To identify novel relevant genes associated with 1q21 gain in Multiple Myeloma (MM)- we have analyzed high-resolution array-CGH profiling to determine the genome-wide copy number amplification (CNA) patterns of the 254 MM samples deposited in the MMRC (Multiple Myeloma Research Consortium) database. Specifically, a systematic method, named Genomic Identification of Significant Targets in Cancer (GISTIC), was designed and used to analyze chromosomal aberrations in cancer [{103}]. Using this approach each marker was scored according to the mean amplitude and frequency of focal amplification across the dataset, and significance values were computed by comparison to the distribution of scores obtained by random permutation of the markers across the genome. Significant peak regions of amplification (or deletion) were identified using an iterative peel-off procedure that distributes the score associated with amplified (or deleted) segments among all peaks that overlap them (weighted according to each peak's score) until no new region crosses the significance threshold of q-value ≤0.25 on each chromosome. By taking into account the auto-correlation within the GISTIC score profiles, we computed for each peak region a confidence interval that is predicted to contain the true driver gene or genes with at least 99% probability. Using this method, we have identified the minimum 1q21 region recurrently amplified in about 40% of MM patients. Then, these results were integrated with expression data of matched MM samples identifying a list of 78 expressed and copy number-driven amplified genes localized in 1q21 that have been enlisted into the screening (**Table 4**).

region	genes in region	genes with copy-number-driven expression (FDR<0.05)	microRNA	known oncogenes	frequency (%)
1q21	**206**	**78**	**4**		**22**
3q26	510	74	14		11
7q32	496	84	16		11
8q24	1	1	0	MYC	11
9q33	4	1	1		29
9q34	14	5	2		27
11q13	2	1	0	CCND1	15
11q23	2	1	0		19
17q23	4	1	0		3
19p13	5	3	0		20

Table 4: Identification of 78 genes with copy-number driven expression of 254 patients in MMRC database.

Bases on this evidence, we performed high-throughput systematic short hairpin RNA (shRNA) approach to identify copy number-driven amplified 1q21 genes whose loss of expression may result in MM cell death and/or growth inhibition. Primary screen was carried out in triplicate using a single-shRNA-per-96 well format. Using this format we were able to obtain an efficiency of transduction up to 70% (range 40-70%) in different established MM cell lines. Specifically, we used 2 different MM cell lines JJN3 and OCI-MY5 carrying c-MAF translocation but with and without 1q21 amplification respectively [{73}]. These two cell lines were infected separately by lentiviral shRNAs using a library of 532 shRNA vectors targeting each of 78 copy number-driven amplified 1q21 genes (Figure 7).

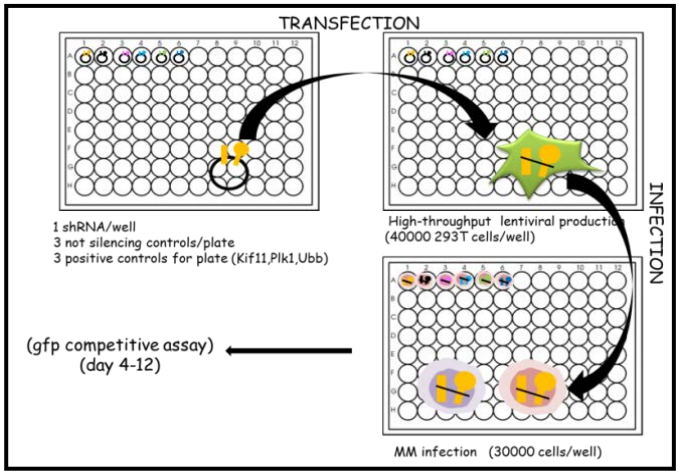

Figure 7: Schematic representation of our high-throughput screening strategy in 96-well format.

After excluding shRNAs that display cytotoxic activity regardless of 1q21 amplification, 1q21 "Achilles hell" vulnerabilities were defined as genes targeted by at least 2 distinct shRNAs, whose downregulation decreased the percentage of GFP-positive MM cells with 1q21 amplification by at least 20% over a 7-day time frame. Specifically, the percentage of GFP-positive cells was evaluated by flow cytometry at day 4 and day 12 after transduction (Figure 8).

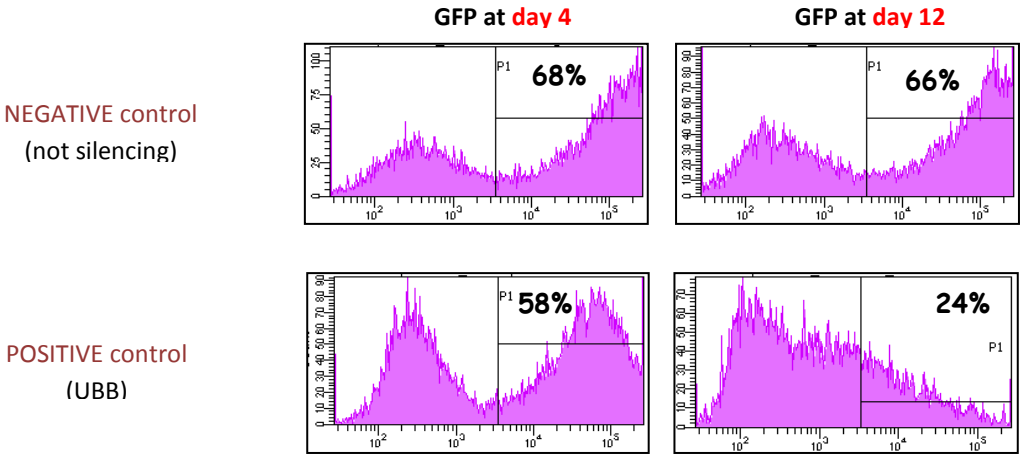

Figure 8: Flow cytometry assay showing four different results of the GFP competitive assay of a representative experiment. Percentage of GFP-positive cells was evaluated by flow cytometry at day 4 and day 12 after transduction.

A shRNA vector delivering a scrambled sequence was included as negative control for each experiment. Using these criteria we were able to eliminate weak and false positive hits from further validation and only strongest hits were selected for secondary validation. Screen performance in terms of sensitivity and reproducibility has been evaluated and standardized by a number of experiments with hairpins silencing either universally or MM-specific essential genes (Figure 9).

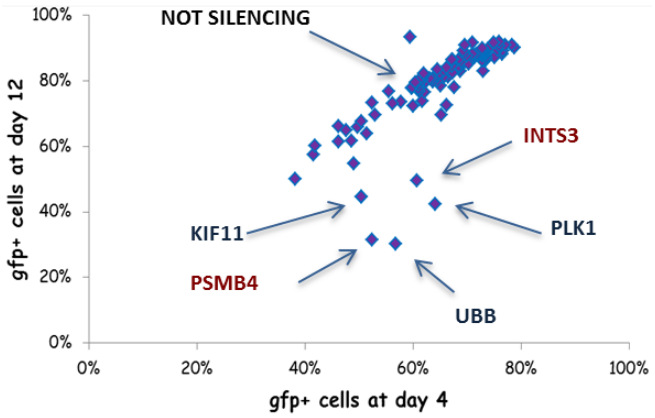

Figure 9: Representative example summarizing the results relative to one 96 well plate used in the high-throughput screening: 91 genes were not silenced by a single hairpin (one/well), instead 3 universally (PLK1, KIF11, and UBB) and 2 MM-specific (PMSB4, INTS3) essential genes showed a decrease in the percentage of GFP positive cells over a frame period of 7 days.

PSMB4 (a well-known MM target)-shRNA was able to impair growth of both JJN3 and OCI-MY5 cells and this confirmed the specificity of our powerful approach. Our primary screen on 78 amplified genes revealed six prime candidates (**Table 5**) implicated in survival or proliferation of MM with 1q21 amplification: MCL1, INTS3, ILF2/NF45, KRTCAP2, UBAP2L, and LASS2. These six genes represented the starting point for further studies.

Genes	Number of shRNAs	Background
MCL1	3	Cell survival, anti-apoptotic factor
INTS3	3	SOSS complex; DNA repair via HR (Rad51 recruitment to DNA damage foci) and ionizing radiation sensitivity
ILF2(NF-45)	2	DNA repair via NHEJ/mitotic control; ionizing radiation sensitivity; IAP1 regulation during the unfold protein response
KRTCAP2	2	regulator of γ-secretase
UBAP2L	2	ubiquitin/proteasome pathway
LASS2	2	ceramide synthase 2, sphingpsine N-acetyl transferase and DNA binding transcription factor

Table 5: List of candidates emerged from the high-throughput screening.

Secondary validation *in vitro* and *in vivo* and prognostic significance

Secondary validation is an essential step for high-throughput shRNA screening experiments, since the level of complexity reached can generate artifacts or non-specific phenotypes. Thus a secondary screen was performed in JJN3 and H929 MM cell lines (harboring 4 copies of the 1q21 amplification but carrying c-MAF and MMSET translocation respectively) [{73}] infected by two different shRNA vectors specific for each of the six genes. First we evaluated the inhibition level of each candidate by Q-RT PCR analysis. The latter confirmed that both shRNAs chosen for the six top genes reduced the expression of the respective mRNA, demonstrating their efficiency (Figure 10).

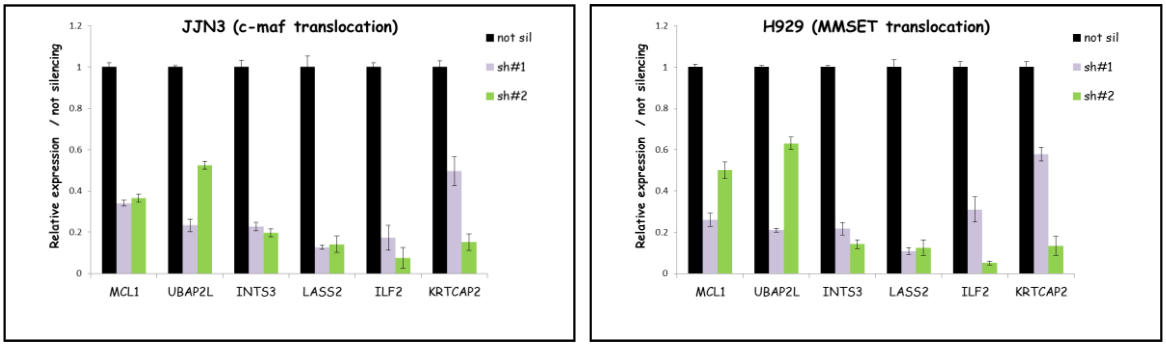

Figure 10: Q-RT PCR analysis showed that shRNA effect correlate with the inhibition level of the 6 targeted genes in JJN3 (left panel) and H929 (right panel).

Moreover, specific assays showed that the each pair of shRNAs specific for the 6 genes affected proliferation/survival and apoptosis of MM cell lines with 1q21 amplification (**Table 6**,Figure 11).

GENE SYMBOL	VIABILITY (%)	APOPTOSIS (%)
Not silenc	93.6 ± 3.2	8.2 ± 0.9
UBB	63.2 ± 4.3	28.3 ± 0.6
MCL1 (sh#1)	61.1 ± 3.1	30.7 ± 2.4
MCL1 (sh#2)	62.9 ± 3.4	33 ± 2.9
INTS3 (sh#1)	81.4 ± 2.4	16.2 ± 2.1
INTS3 (sh#2)	79.3 ± 3.4	22.8 ± 3.2
UBAP2L (sh#1)	85.7 ± 4.3	17.7 ± 1.7
UBAP2L (sh#2)	85.2 ± 2.1	11.4 ± 1.7
LASS2 (sh#1)	76.5 ± 1.5	13.3 ± 2.1
LASS2 (sh#2)	85.1 ± 2.1	13.1 ± 2.3
KRTCAP2 (sh#1)	85.3 ± 3.2	11.8 ± 1.5
KRTCAP2 (sh#2)	81.1 ± 3.4	16.4 ± 0.9
ILF2 (sh#1)	85.5 ± 2.1	13 ± 0.4
ILF2 (sh#2)	78.5 ± 2.3	14.7 ± 0.8

GENE SYMBOL	VIABILITY (%)	APOPTOSIS (%)
Not silenc	86.7 ± 3.22	10.6 ± 1.4
UBB	47.1 ± 3.7	42.1 ± 0.6
MCL1 (sh#1)	38.5 ± 5.2	58.2 ± 1.3
MCL1 (sh#2)	67.3 ± 3.9	25.3 ± 1.1
INTS3 (sh#1)	80.2 ± 2.1	18.1 ± 3.1
INTS3 (sh#2)	79.5 ± 4.4	19.4 ± 2.6
UBAP2L (sh#1)	80.1 ± 1.3	18.2 ± 3.7
UBAP2L (sh#2)	86.1 ± 1.8	11.4 ± 2.2
LASS2 (sh#1)	79.1 ± 2.6	15.4 ± 3.2
LASS2 (sh#2)	78.6 ± 1.9	16.2 ± 3.1
KRTCAP2 (sh#1)	83.3 ± 3.6	12.8 ± 1.5
KRTCAP2 (sh#2)	80.1 ± 2.1	17.8 ± 1.1
ILF2 (sh#1)	81.2 ± 2.7	15.3 ± 3.1
ILF2 (sh#2)	78.5 ± 3.6	17.8 ± 2.9

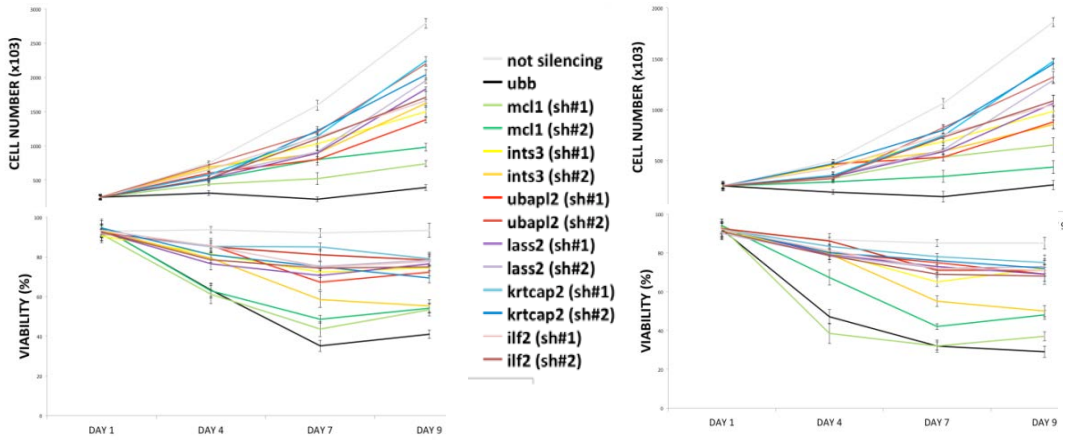

Table 6-Figure 11: Secondary validation by high-titer virus in JJN3 (lower panels and table on the left) and H929 (lower panels and table on the right) indicating the shRNA effects on cell viability and apoptosis. We also included two shRNA vectors as negative and positive controls. Cell viability and apoptosis were measured by Trypan Blue exclusion assay and Annexin V staining, respectively.

The clinical relevance of our genes is critical to figure out their potential prognostic impact. For this purpose we decided to analyze the correlation between gene expression profiling (GEP) and survival data of 256 MM patients with high-dose melphalan treatment followed by tandem autologous transplantation included in the Arkansas database. After excluding MCL1, a well known MM survival factor [{104}], we highlighted that only 2 of 5 targeted genes, ILF2/NF-45 (p=0.0156) and UBAP2L (p=0.00552) were significantly related with the clinical outcome (Figure 12).

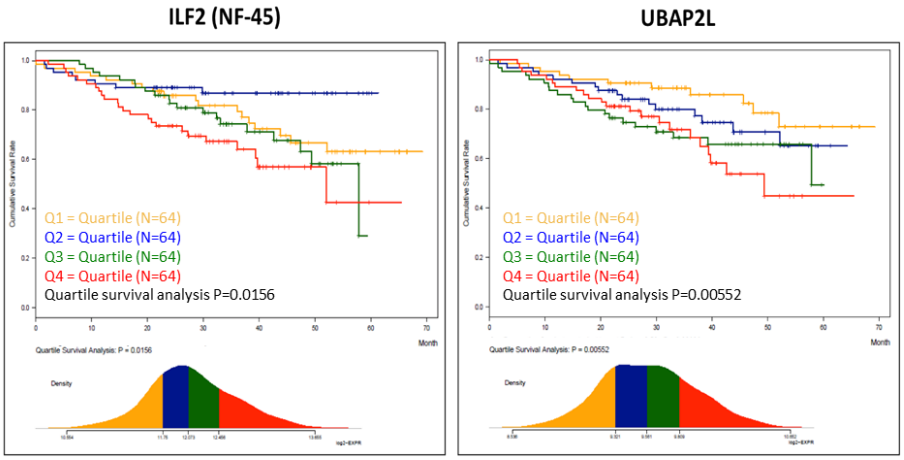

Figure 12: Kaplan-Meier analysis on 256 patients treated with high-dose Melphalan and tandem autologous transplantation on the six genes emerged from the high-throughput screening.

Furthermore the tumorigenic potential of JJN3 and H929 infected with the 2 shRNAs for the 5 genes was determined in NOD-SCID (non-obese diabetic severe combined immunodeficiency) mice by a sub cute injection. A group of mice injected with the two MM cell lines ($2x10^6$cells/mice; 5 mice/group) carrying the control shRNA was included in each experiment too. Control JJN3 cells were able to develop tumors and kill the 100% of the mice within less than 30 days. Instead H929 cells needed almost 50 days (Figure 13). Our approach demonstrated that only the knockdown of ILF2 increased the survival of NOD/SCID mice injected with either JJN3 or H929 cells (shRNA 1: p=00.3 and p=0.01; shRNA 2: p=0.03 and p=0.01, respectively). Therefore, our study was restricting towards ILF2 (NF-45) as candidate gene.

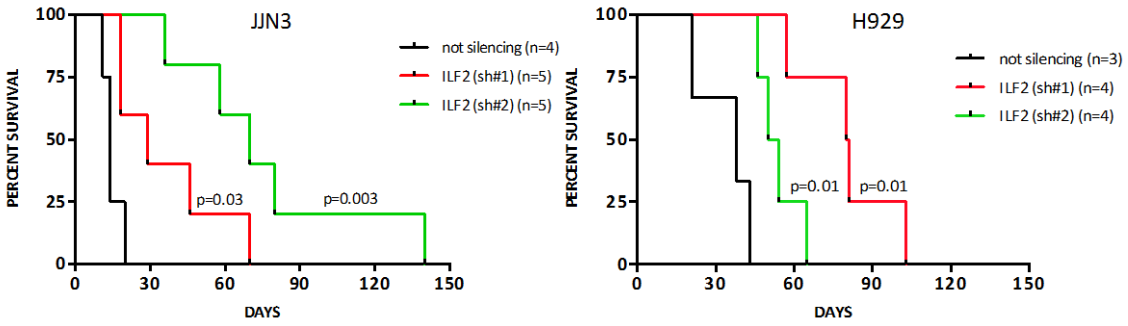

Figure 13: Survival curves of NOD-SCID mice sub cute injected with control or ILF2 shRNA infected JJN3 cells (left panel) and with control or ILF2 shRNA infected H929 cells (right panel).

ILF2 (NF45): DNA damage, splicing and genomic instability

Since we restricted our studies on ILF2 gene, further analyses focused to understand its potential role in survival of MM cell lines carrying 1q21 amplification. Thus we submitted a RNA sequencing analysis to investigate which pathways were deregulated following ILF2 knockdown in JJN3 cell line. The most significant pathways up-regulated or down-regulated in ILF2 shRNA2 compared to control samples are resumed on Figure 14. We could appreciate a dysregulation of cell cycle, RNA metabolism, and RNA splicing, telomere and chromosome maintenance pathways.

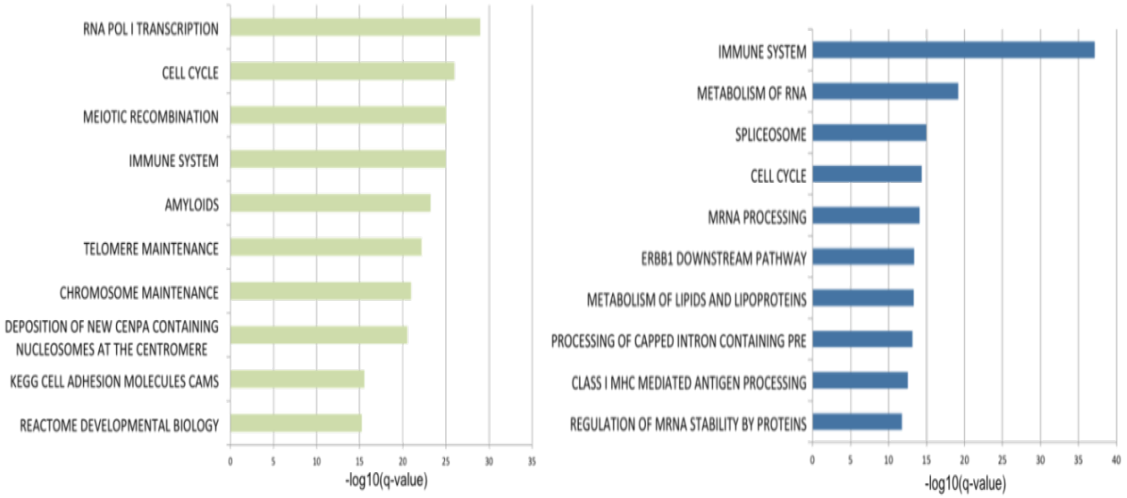

Figure 14: Pathways significantly upregulated (right panel) and downregulated (left panel) emerged from RNA-sequencing analysis in ILF-2 knockdown JJN3 cells. Each sample processed in duplicate.

The cell cycle alteration was also confirmed by FACS analysis on JJN3 cell line, with and without ILF2 knockdown (Figure 15A). As reported in literature, we observed that JJN3, a p53-deficient cell line, rely on checkpoint kinase 1 (Chk1) to arrest cell-cycle progression in the S and G2 phases [{102}]. Indeed H929, a p53 wild type cell line, showed a stop in G1 phase of cell cycle (Figure 15B). Analyzing in detail the RNA sequencing data we also found a large number of proteins involved in DNA damage pathway.

JJN3	% Sub-G0	% G0/G1	% S-phase	% G2
Not silenc	2.34 ± 0.11	42.55 ± 0.27	50.12 ± 0.16	7.32 ± 0.35
Ilf2-1 sh#1	4.91 ± 0.54	43.27 ± 0.41	40.03 ± 0.42	16.69 ± 0.71
Ilf2-2 sh#2	6.19 ± 0.17	38.59 ± 0.07	40.36 ± 0.57	21.04 ± 0.64

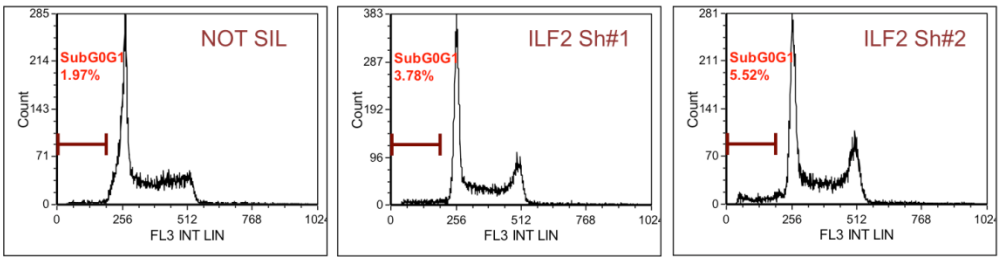

H929	% Sub-G0	% G0/G1	% S-phase	% G2
Not sil	3.69 ± 0.25	56.4 ± 0.43	30.85 ± 0.45	12.75 ± 0.63
Ilf2-1 sh#1	4.87 ± 0.36	65.55 ± 0.32	24.32 ± 0.67	10.13 ± 0.23
Ilf2-2 sh#2	6.92 ± 0.65	72.52 ± 0.91	18.48 ± 0.34	9.01 ± 0.25

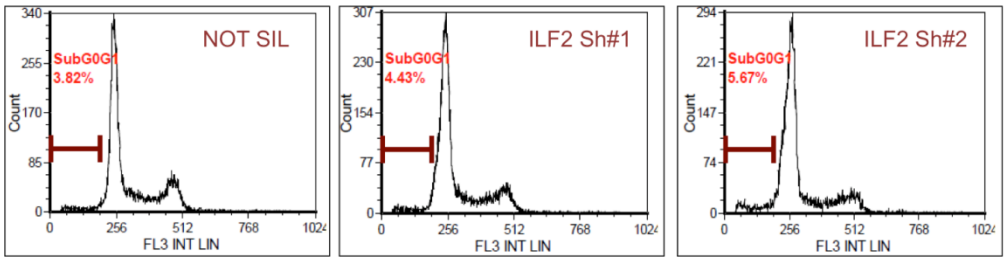

Figure 15: Flow cytometric analysis of cell cycle distribution following not silencing and the two ILF2 shRNAs transduction in JJN3 and H929 cells (upper and lower panel).

Synergistic effect between DNA damage agents and ILF2 knock-down

Based on RNA sequencing analysis data, we decided to evaluate the DNA signaling response activation and apoptosis level after knockdown of ILF2 in MM cells. Western blotting analysis on JJN3 and H929 cells, showed that the two different shRNAs, ILF2Sh#1 and ILF2Sh#2, have different efficiency in ILF2 down regulation, and this effect is directly proportional to the level protein decrease of its partner ILF3 (existing in two different isoforms NF90 and NF110). At the same time, ILF2 protein level was inversely proportional to the amount of DNA damage signaling, DNA damage response (γH2AX, phospho-ChK2, phospho-ATM, phospho-ATR, and phospho-DNAPK) and Cleaved Caspase 3, a well-known marker of apoptosis. Therefore Western Blot and immunofluoresecence analyses suggest that MM cells depleted of ILF2 accumulate DNA damage more easily than the control cells. This trend is confirmed also by the increasing of gigantic cells in ILF2 knock-down JJN3 cells versus the control ones (Figure 16).

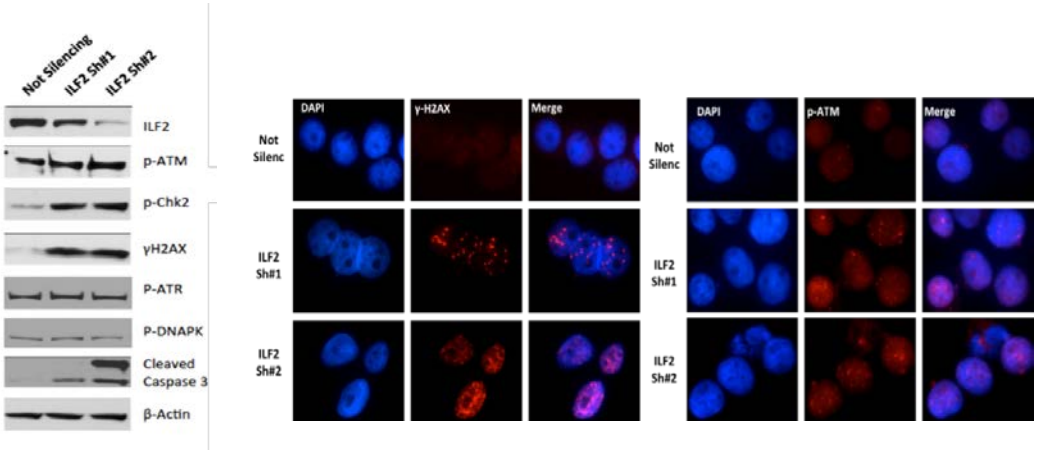

Figure 16: WB analysis for the DNA damage signaling in JJN3 MM cell line was examined 7 days after not silencing and shRNAs infection. β-actin was included as control for equal loading (left panel). Localization of γH2AX and p-ATM nuclear foci in single cells was determined 7 days after JJN3 infection. Image acquisition was performed by confocal microscopy and post-processing analysis of the images was processed using ImageJ software (right panel).

Binucleation or multinucleation together with Abnormal Nuclear Morphologies (ANMs) are very good markers of genomic instability and malignancy. MM ILF2 depleted cells showed a significantly higher number of binucleated and multinucleated cells together with nucleoplasmic bridge, micronuclei and nuclear buds (ANMs) (Figure 17) due to DNA damage activation and DNA repair defects.

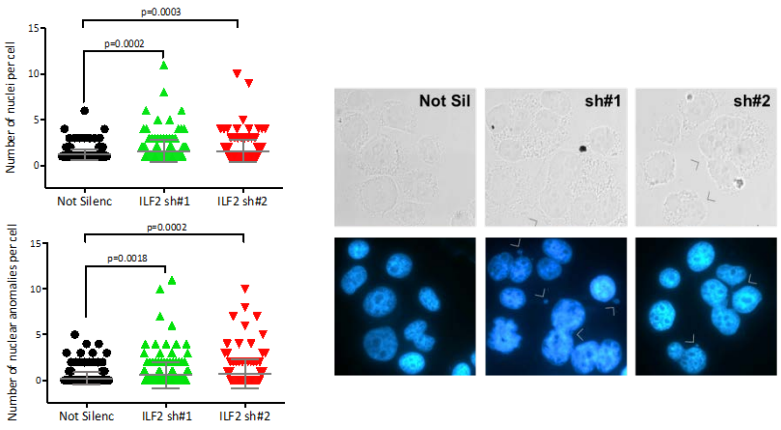

Figure 17: ILF2 knockdown in JJN3 resulted in multinucleated phenotypes and abnormal nuclear morphologies (ANMs) indicated by arrowheads (right panel). The number of nuclei and ANMs per cell is plotted (left panel).

Accumulation of γ-H2AX foci, features of genomic instability, together with increased apoptosis, could represent an important chance in perspective of cancer treatment, especially for those subgroups of patients unresponsive to chemotherapy. To this end, we tried to evaluate if the downregulation of ILF2 in MM cells could increase sensitivity to DNA damage agents. We decided to treat Not Silencing, ILF2#1 and ILF2#2 JJN3 cells with Melphalan, a nitrogen mustard still in use to treat MM patients. Thus, we tried to figure out the molecular pathway activation during drug exposure. We treated Not Silencing and ILF2#2 JJN3 cells with 25μM Melphalan for 12 hours and, at the indicated time points, we collected proteins to perform Western blot analysis on DNA damage signaling, DNA damage response and apoptotic pathways (Figure 18). We observed a significant increase of γH2AX phosphorylation in ILF2#2 samples compared to the control, especially at later time point. On the contrary, the activation of phospho-ATM and phospho-NBS1 in ILF2#2 sample seemed weaker overtime rather than Not Silencing one. Finally Caspase3 confirmed a stronger apoptosis in ILF2#2 respect Not Silencing cells. Quantification of the protein signal together with statistical analysis, clearly confirmed the synergistic effect of Melphalan and ILF2 shRNA on JJN3 cells, probably due to an impaired activation of DNA damage response (Figure 18).

To confirm this hypothesis, we designed a drug exposure time point, with the same concentration of Melphalan but, this time, we washed out the drug after 6 hours of treatment, to follow the cell ability to recover DNA damage (Figure 18). How expected, at starting point the γH2AX content was higher in ILF2#2 respect Not Silencing sample and was increasing, having different absolute content, with almost the same kinetics after drug exposure in both samples. After Melphalan washed out, the activation of the DNA damage response in ILF2#2 resulted once again wicker respect to control JJN3 cells from 6 to 10 hours, getting even worst after 10 hours (Figure18). As a result of this impairment, we observed a certain quantity of unrepaired DNA damage in ILF2 knocked down respect to control cells (Figure 18).

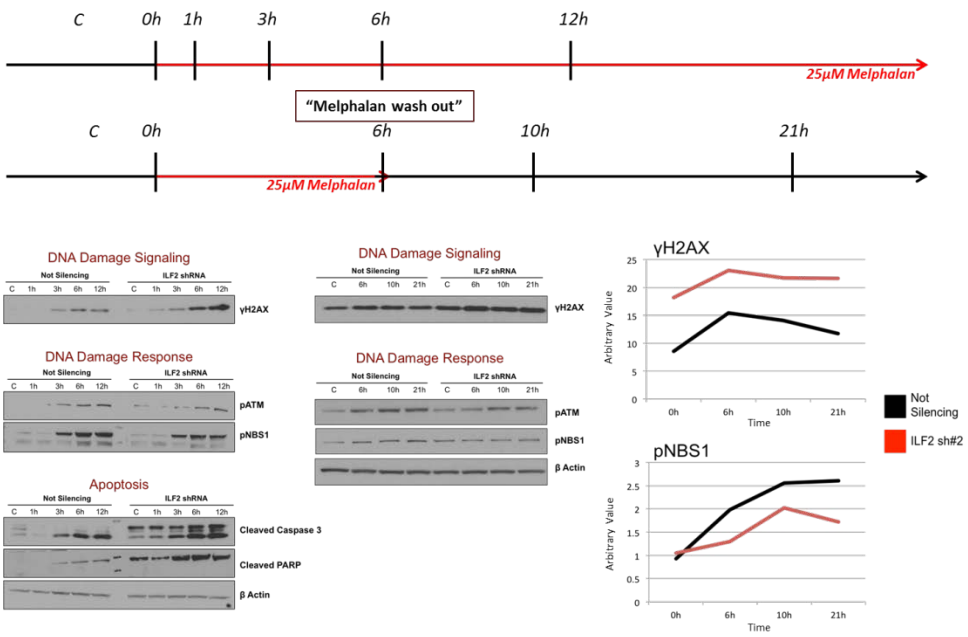

Figure 18: Schematic representation of the two different time courses (upper panel). WB analysis of the expression of activated forms (γH2AX, p-ATM, p-NSB1) of mediator DNA damage proteins and protein involved in the apoptosis process (Cleaved Caspase 3, Cleaved PARP) in JJN3 MM cell line was examined after Melphalan 25μM with or without wash-out. B-actin was included as control for equal loading (lower left and middle panels). Densitometric analysis to evaluate protein amount was performed using ImageJ software (lower right panels).

At the opposite side, in a regimen of ILF2 overexpression, the accumulation of γH2AX foci was significantly reduced and after 12 hours of Melphalan treatment, myeloma cells seemed protected from apoptosis, like indicated by decreasing of cleaved caspase-3 protein (Figure 19).

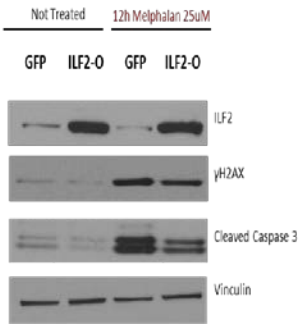

Figure 19: WB analysis of ILF2, γH2AX and Cleaved Caspase-3 following ILF2 overexpression (ILF2-O) with and without Melphalan treatment. JJN3 cells infected with a GFP vector were included as a control (GFP). Vinculin was included as control for equal loading.

ILF2 interacts with proteins involved in DNA damage response, RNA metabolism and splicing

Trying to figure out the reason why ILF2 knock out can affect the DNA damage response of MM cells, we performed an ILF2 immunoprecipitation (IP) in Not Treated and in 25μM Melphalan Treated JJN3 cells after 10 hours of treatment and we submitted those samples for a mass spectrometric analysis (Figure 20). To obtain a reliable list of potential ILF2 partner proteins, we only considered peptides that not appeared in the Immunoglobulin control lane. We found almost not differences between Not Treated and Treated JJN3 cells in terms of ILF2 potential binding proteins.

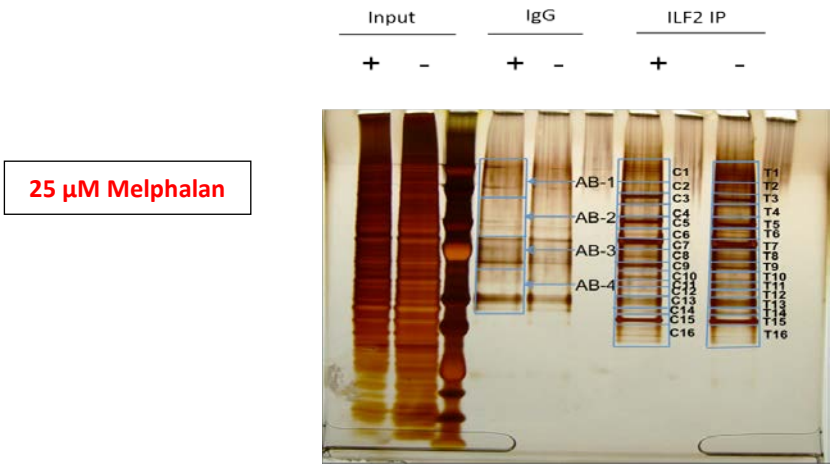

Figure 20: Separation of proteins by SDS-PAGE. SILAC-labeled cell proteins were separated on a 4-12% Agarose gel and stained with the Silver Stain Kit for Mass Spectrometry (Pierce®). The grids overlaid on the ILF2 IP samples demonstrate the area taken for individual slices. We excluded from the sampling the peptides also presented in the Input lane.

In order to validate the candidates, we did a Western blot analysis on ILF2-IP to confirm the interactions in wild type JJN3 cells. We got a positive outcome for both of ILF3 isoforms (NF90/110), known ILF2 interacting partners [106-107]. We saw that ILF2 interacts with a panel of different RNA proteins (RBPs) including Nucleophosmin (NPM), Y-box-binding-protein1 (YB-1), Nucleolin, Adenosine Deaminase Acting on RNAs (ADAR1), Sam68 and a couple of heterogeneous nuclear ribonuclearproteins (hnRNPs), A1, U like, K, C1/C2, F/H, G, which protect cells from DNA damage directly at the site of the damage or indirectly stabilizing specific pre-mRNAs [105](Figure 21).

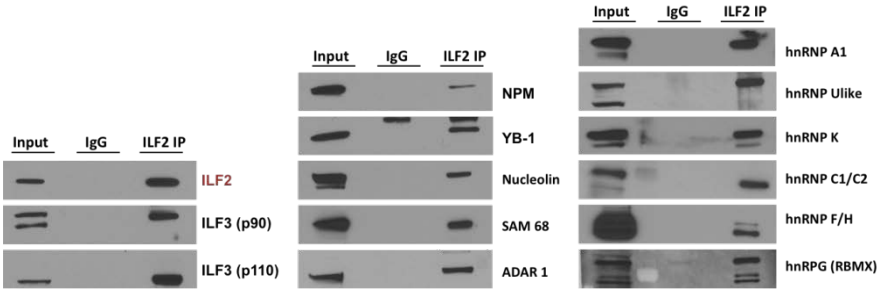

Figure 21: Validation by Immunoprecipitation of the mass spectrometry top scoring candidates in JJN3 wild-type cell line.

To evaluated if ILF2 is required to ensure alternative splicing and processing of specific pre-mRNAs in physiological conditions, the RNA-Sequencing analysis of JJN3 cells carrying shRNA targeting ILF2 displayed a specific aberrant RNA splicing pattern associated with ILF2 down-regulation, detecting 646 differential splicing events for 500 genes, among which 46.5% are predicted to produce loss-of-function transcripts that arise mainly due to a premature stop codon or an in-frame deletion disrupting known functional domains. Interestingly, the differentially spliced transcripts associated to ILF2 downregulation are enriched in genes directly involved in different DNA damage repair pathways, including single-strand base excision, single-strand mismatch, double-strand non homologous and homologous repair (Figure 22). These data emphasize our conviction on a link between ILF2 and DNA damage regulation.

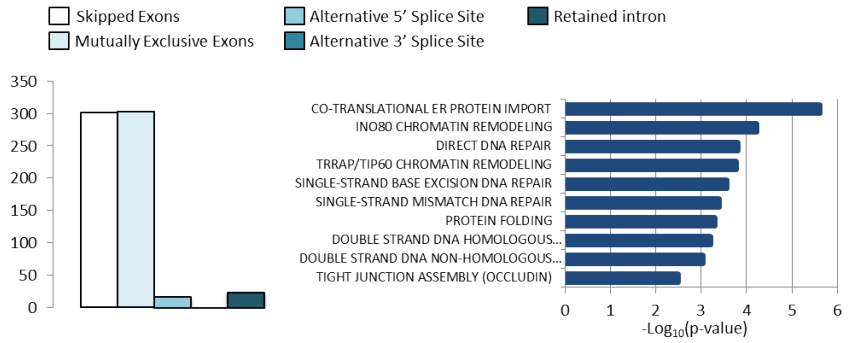

Figure 22: RNA-sequencing analysis on JJN3 cells with ILF2 knock-down detected a specific aberrant RNA splicing pattern.

Interestingly, RNA-Sequencing analysis of JJN3 cells under Melphalan treatment displayed different RNA splicing events, not emerged from the previous one, associated

with DNA damage activation, detecting 1,363 differentially splicing events for 989 genes, mostly involved in the DNA repair of several classes of DNA damage, sister chromatid cohesion, cell cycle regulation and mRNA processing pathways, consistent with our hypothesis that ILF2 might promote splicing events after DNA damage activation (Figure 23).

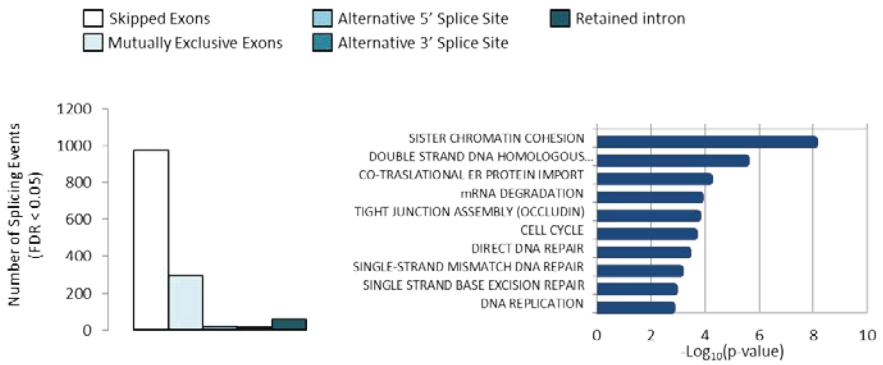

Figure 23: RNA-Sequencing analysis of JJN3 cells with ILF2 knock-down treated with Melphalan detected new splicing events associated to DNA damage.

ILF2 regulates YB-1 nuclear translocation

As ILF2 and ILF3 interact with RNA and contributes to RNA gene regulation at the levels of transcription, splicing, export and translation [{118}], to check if ILF2 down-regulation could affect protein translation or stability of its partners, we treated Not Silencing and ILF2sh#1 and sh#2 with 25µM Melphalan for 10 hours and we analyzed their protein levels by Western blot. With the exception of ILF3 p110 isoform, which showed a translational modulation proportional to the amount of ILF2 protein abrogated by the two different shRNAs, the ILF2 knock-down with or without Melphalan treatment did not modify ILF2 interactome suggesting that ILF2 does not bind alternative partners during DNA damage conditions (Figure 24).

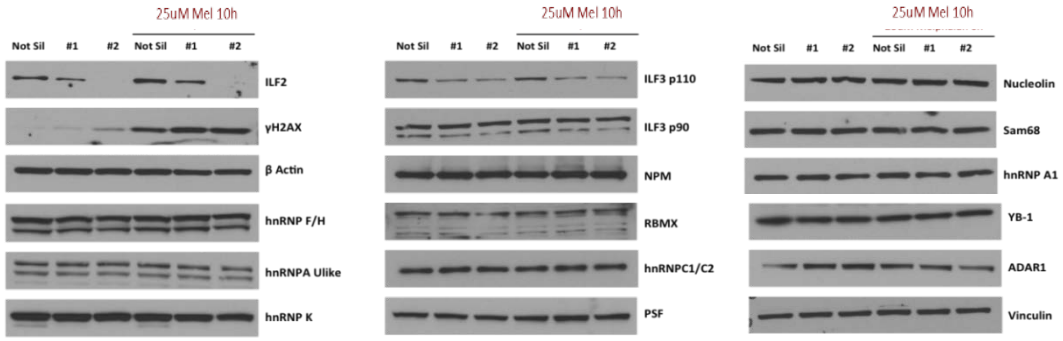

Figure 24: Western blot of ILF2 interactome with and without Melphalan treatment. B-actin and vinculin were included as control for equal loading.

Since some of ILF2 interacting proteins, like Nucleolin, YB-1 and Sam68 are known to shuttle between cell cytoplasm and nucleolus when DNA damage occurs [{105}], we checked if ILF2 knock-down could affect their dynamic localization by immunofluorescence. We treated again Not Silencing and ILF2sh#2 JJN3 cells with Melphalan, as described above, and we stained cells with anti γH2AX antibody, as DNA damage marker, looking for impaired localization of this ILF2 partners before and after DNA damage. We found no change in localization between Not Silencing and ILF2sh#2, before and after Melphalan treatment, for almost all the tested proteins discovered to bind ILF2, except for YB-1. Looking at Y-box-binding-protein 1 by wide-field microscopy in fact, we observed an increase of this protein in Not Treated JJN3 cell nuclei after DNA damage induction. Instead under the same condition, no YB-1 nuclear signal was detected before and after the DNA damage in the ILF2sh#2 JJN3 cells (Figure 25).

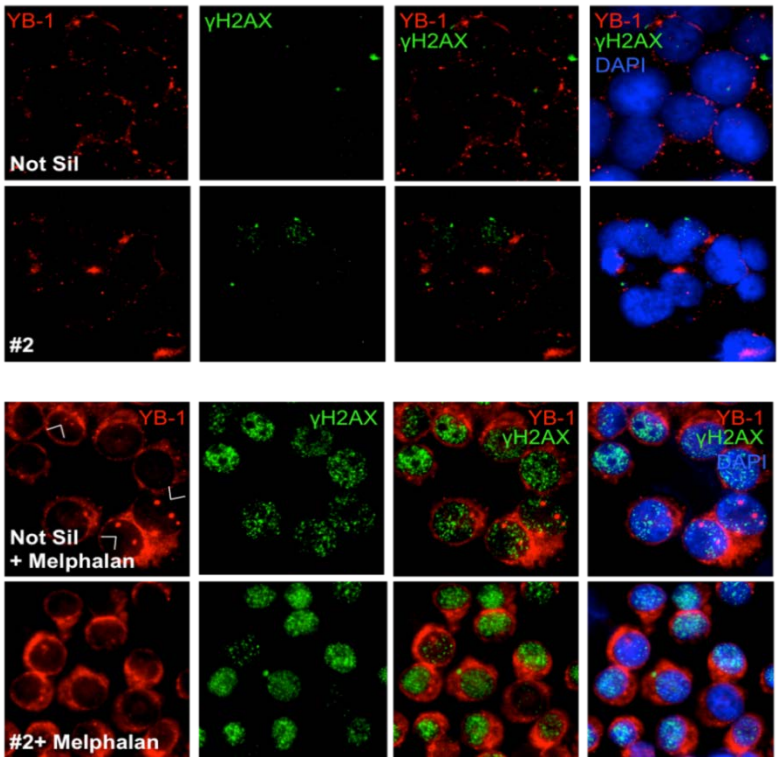

Figure 25: Localization of γH2AX and YB-1 foci in single cells was determined at 10 hours with (lower panel) and without (upper panel) Melphalan treatment. Image acquisition was performed by wide-field microscopy and post-processing analysis of the images was processed using ImageJ software.

Moreover, to assess what we observed by wide-field microscopy we decided to stain JJN3 Not Silencing and shILF2#2, with ILF2 and YB-1 antibody and to analyze the localization of these proteins by confocal microscopy. In the control cells, ILF2 presented a staining almost nuclear and diffuse, shifting in brilliant dots after DNA damage. In the same cells instead, YB-1 was almost cytoplasmic, with few nuclear discrete dots that definitely increased after Melphalan. Finally, the shILF#2 staining permanently demonstrate that no YB-1 protein can be recruited in the cell nuclei of MM cells after DNA damage (Figure 26).

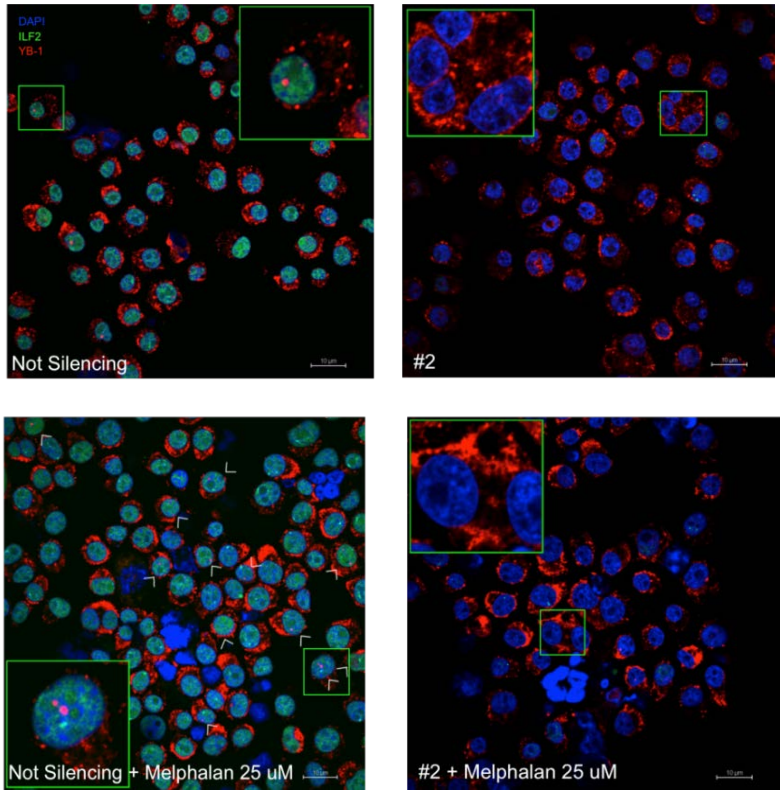

Figure 26: Localization of ILF2 and YB-1 nuclear foci in single cells determined at 10 hours with (lower panel) and without (upper panel) Melphalan treatment. Image acquisition was performed by confocal microscopy and post-processing analysis of the images was processed using ImageJ software. The scale bar represents 10µm.

To examine closely the impaired YB-1 localization induced by ILF2 knockdown, we decided to perform a cytoplasm-nuclear fractionation Western blot, in Not Silencing and ILF2#2 JJN3 cells, before and after Melphalan treatment. Not Silencing control cells showed that, as expected, YB-1 is able to translocate to the nucleus after DNA Damage and, surprisingly, also ILF2 showed the same behavior. On the contrary after ILF2 knock-down (ILF2 sh#2 sample), the nuclear quantity of YB-1 protein held steady before and after DNA Damage (Figure 27). Then, we wondered what would have happened to this protein shuttling, after the same treatment with Melphalan, but in a setting of ILF2 overexpression. We over expressed ILF2 protein in JJN3 cells and we repeated the same experiment checking again, by Western blot, the YB-1 and ILF2 nuclear protein amount before and after DNA damage. As expected, the control showed similar results for the Not Silencing control cells previously used. Interestingly at the opposite side, the overexpression of ILF2 was quite completely cytoplasmic and, as is shown in Figure 27,

strongly enhanced the YB-1 nuclear translocation after DNA Damage induction. Finally we can conclude that under Melphalan treatment YB-1 nuclear translocation was impaired in ILF2 depleted cells and was potentiated after ILF2 overexpression.

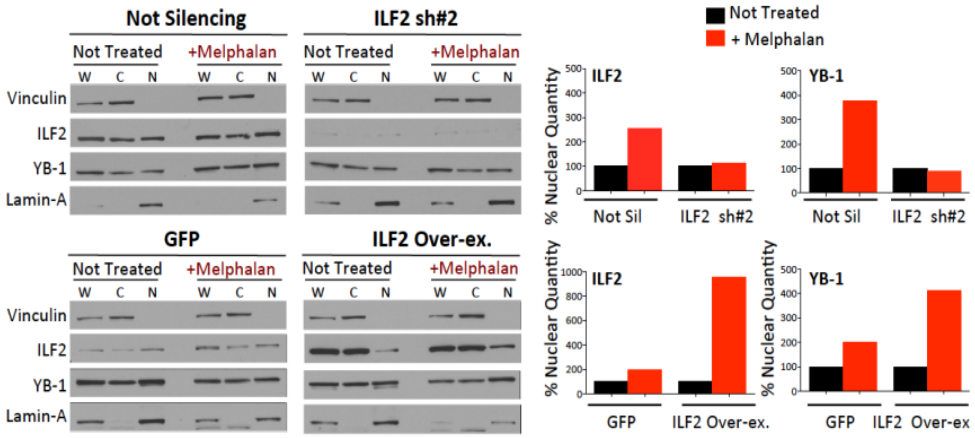

Figure 27: Cytoplasm-nuclear fractionation Western blot on JJN3 cell line infected with scrambled construct (Not Silencing) and ILF2 sh#2, and with GFP and ILF2 overexpressed vectors (left panels). Vinculin and Lamin-A were included as control for equal loading on the whole and nuclear protein extracts respectively. Densitometric analysis to evaluate the protein loading performed using ImageJ software is presented on the right side.

Discussion

Despite significant efforts towards the development of risk stratification strategies for patients with Multiple Myeloma (MM), the capacity to molecularly predict the natural history of these patients is still limited. Many studies have shown that genetic alterations especially t(4;14) translocation, loss of the short arm of chromosome 17 and amplification of chromosome 1q21 are associated with poor outcome and represent independent adverse predictors of shorter progression-free survival (PFS) and overall survival (OS)[{39; 108}]. The 1q21 amplification is among the most frequent chromosomal aberrations in patients with myeloma and is considered a very poor-risk genetic feature that is especially correlated with disease progression and drug resistance [{73; 75; 76}]. Although the 1q21 locus contains a large number of possible candidate genes that are related to disease pathogenesis including PSMD4, CKS1B, BCL9, MCL1, MUC1, PDZK1 [{80;72; 111-112; 109; 104; 113-116}], so far the relevant genes on 1q21 remain unclear and the absence of focal amplifications involving this region strongly suggests that more than a single candidate may represent the driver event responsible for poor outcome in this group of myeloma patients in response to different therapeutic regimens. Thus this study focused first on the identification of critical 1q21 "Achilles heels" vulnerabilities for MM, then on their functional validation. Our in-depth bioinformatics analysis of MM genome has generated a high priority list of 78 amplified and overexpressed genes localized in 1q21 (**Table 7**). These genes have been enlisted into a systematic shRNA screen *in vitro* to identify critical 1q21 candidates whose loss of function results in the selective death and/or growth inhibition of MM cells carrying the 1q21 amplification and c-MAF translocation (JJN3 cell line) but not in MM cells without 1q21 amplification (OCI-MY5 cell line) [{73}] (Figure 7). With our 96-well high-throughput screening strategy, six genes were emerged as key 1q21 targets; MCL1, INTS3, ILF2, KRTCAP2, UBAP2L, LASS2. Secondary validation experiments in the MM cell lines JJN3 and H929 (harboring 4 copies of the 1q21 amplicon) [{73}] confirmed for all the six candidates by two different shRNAs the quality of our approach (Figure 10) and mainly the impairment of cell proliferation/survival and apoptosis (Figure 11 and **Table 6**). Thus our efforts have been directed forward the functional validation of the six hits resulted from our preliminary screen. After excluding MCL1 gene, known factor implicated in myeloma cell survival[{104}], the subsequent studies on the remaining five candidate genes have pointed out a potential role of ILF2/NF45 in DNA damage response and RNA splicing in 1q21 amplification context.

Interleukin enhancer binding factor 2 (ILF2), also named NF45, belongs to the NFAT (Nuclear Factor of Activated T cells) complex in a heterodimeric core with ILF3 (NF90/NF110) that is widely expressed in many cell-types and tissues [118]. ILF2 shows a predominant expression in the nucleus mostly in testis, brain, and kidney but it results overexpressed in Lymphoma and Leukemia transformed cell lines [119]. ILF2 interacts with numerous proteins and RNAs partecipating in transcription, RNA transport, mRNA stability, and translation [118]. Apart from regulation of mRNA metabolism, ILF2 has been implicated in the regulation of other pathways including DNA damage response[118; 120], microRNA processing [121] and viral infection [122; 123].

In our study, the target validation of ILF2 in NOD-SCID mice showed that ILF2 down-regulation had a significant impact on *in vivo* survival of JJN3 and H929 cell lines (Figure 13). Therefore, we sought to further characterize the ILF2 role in 1q21-amplified myeloma. As shown in other systems [106; 118], myeloma cells depleted for ILF2 displayed giant multinucleated cells and abnormal nuclear morphologies (nucleoplasmic bridges, nuclear buds and micronuclei). Such mitotic defects and aberrant morphologies are linked to the disruption of genomic integrity due to DNA damage activation and DNA repair defects. Following ILF2 down-regulation we observed a significant activation of the ATM-dependent signaling pathway, but differently from other findings on different cellular systems [118; 120], it resulted ATR and DNA-PK independent (Figure 16). Notably, we observed also an accumulation of γH2AX foci (Figure16), consistent with an accumulation of DSBs (Double Strand Breaks), which led to cell cycle arrest either in G2/M or in G0/G1 (Figure 15), depending on TP53 status [102] (absent in JJN3 and wild-type in H929, respectively) and Caspase 3-mediated apoptosis (Figure 16).

Thus, to determine whether ILF2 is involved in the regulation of DNA damage signaling and DNA repair pathways in MM cells with 1q21 amplification, we evaluated if ILF2 down-regulation increased myeloma sensitivity to DNA-damaging agents. Employing Melphalan treatment as activator of DNA damage signaling, ILF2-depleted MM cells subjected to continuous Melphalan treatment showed synergetic accumulation of phospho-H2AX foci and increased caspase-3-induced apoptosis (Figure 18). Similar results were obtained in drug wash-out experiments, in which the kinetics of DNA damage foci resolution was evaluated following Melphalan withdrawal (Figure 18). Our findings indicated that ILF2 down-regulation was be able to potentiate Melphalan-induced DNA

damage activation and apoptosis in JJN3 cell line. Conversely, further increase of ILF2 expression significantly reduced the accumulation of phospho-H2AX foci and protected MM cells from Melphalan-induced apoptosis (Figure 19).

Although several studies indicated an association between ILF2 and cancer, the detailed role and mechanism are still unknown [{124-126}]. Recently, it was reported that ILF2 over-expression predicted poor survival in non-small cell lung cancer and in glioma [{127-128}]. Accordingly, our clinical correlative studies showed that higher levels of ILF2 expression correlated with poor survival of MM patients treated with high-dose Melphalan followed by tandem autologous transplantation ($p=0.0156$, Figure 12).

Collectively, these data support the view that ILF2 is involved in the regulation of DNA damage response pathways and are consistent with its role as a mediator of double-strand DNA break repair. To understand the molecular mechanisms underlying the involvement of ILF2 in DNA damage response in MM cells, we performed ILF2 immunoprecipitation experiments combined with mass spectrometry in the JJN3 cell line (Figure 20). Further validation of ILF2 interactome confirmed that beside its known binding partners NF90/NF110, ILF2 interacts with numerous RNA binding proteins (RBPs) including NPM, YB-1, nucleolin, ADAR1, and various heterogeneous nuclear ribonucleoproteins (hnRNPs), which are directly involved in DNA repair, maintenance of genome stability, and regulation of DNA damage response by modulating alternative splicing and stability of specific pre-mRNAs (Figure 21) [{105}]. Thus, we first evaluated if ILF2 is required to ensure alternative splicing and processing of specific pre-mRNAs in physiological conditions. The RNA-Sequencing analysis on JJN3 cells carrying shRNA targeting ILF2, displayed differentially spliced transcripts directly involved in DDR (DNA Damage Response) of several types of DNA damage, including single-strand base excision, single-strand mismatch, double-strand non homologous and homologous repair, supporting the tight connection between ILF2 and DNA damage regulation (Figure 22), as previous studies reported in different systems [{118; 120}].

Since recent studies reported that DNA damage affects splicing decision up- or down-regulating a significant fraction of m-RNAs through modulation of the interactions between RBPs and their target mRNA molecules modifying mRNA stability [{129-130}], we determined following exposure to Melphalan treatment if ILF2 is recruited to promote splicing events after DNA damage activation. Indeed RNA-Sequencing analysis of JJN3

cells treated with Melphalan and depleted for ILF2, showed different RNA splicing events associated with DNA damage activation, mostly involved in the DNA repair of several classes of DNA damage, sister chromatid cohesion, cell cycle regulation and mRNA processing pathways (Figure 23), accordingly with previous findings where RNA metabolism and DNA repair pathways are functionally crossed [{130}].

Next, to determine the mechanistic bases of how ILF2 down-regulation impairs RNA splicing of DNA repair genes both in physiological condition and after DNA damage activation, we evaluated if ILF2 is required for the stability or nuclear localization of its interactors, which may shuttle from the cytoplasm to the nucleus in response to DNA damage [{105}]. ILF2 down-regulation was associated with a dramatic post-transcriptional destabilization of its partner NF110 without affecting NF90 or RBP and hnRNP levels (Figure 24) and significantly impaired the nuclear localization of YB-1 after Melphalan treatment (Figure 25-27) without modifying the subcellular localization of the other interacting proteins. Notably, further increase of ILF2 expression strongly activated YB-1 nuclear localization after DNA damage treatment (Figure 27).

These findings demonstrate that ILF2 levels modulate the nuclear localization of YB-1 in response to DNA damage and gain added significance in light of recent findings showing that YB-1 contributes to disease progression, survival, and drug resistance in MM cells [{131}].

Although it was reported that the aberrant up-regulation of ILF2 expression could be associated to a malignant phenotype in Leukemia and Limphomas [{119}], as well as it is known that ILF2 is involved in several tumors including breast cancer, lung cancer, glioma, HCC and colorectal cancer [{126-128; 131-134}], further studies are necessary to figure out better its role. Notably, to date the role of ILF2 in MM has not been yet investigated. Therefore, all these data provide evidence that ILF2 is a novel 1q21 gene target in MM with a pivotal role in DNA damage repair and in the localization of YB-1. Importantly, our findings raise ILF2 in a critical position for the regulation of physiological and DNA damage-induced mRNA splicing process. In summary, we believe that ILF2 might be a novel therapeutic target to enlist into prognostic and drug discovery efforts for a more effective classification and management of MM patients with 1q21 amplification who do not benefit from recent treatment improvements.

Bibliography

[1]: Kuehl W. M. and Bergsagel P. L. Multiple myeloma: evolving genetic events and host interactions. *Nature Review Cancer.* 2002; 2: 175-187.

[2]: Kyle R.A., Gertz M.A., Witzig T.E., Lust J.A., Lacy M.Q., Dispenzieri A. et al. Review of 1027 patients with newly diagnosed multiple myeloma. *Mayo Clinic Proceedings.* 2003; 78: 21-33.

[3]: Lynch H. T., Watson P., Tarantolo S., Wiernik P. H., Quinn-Laquer B., Isgur B. K., et al. Phenotypic heterogeneity in multiple myeloma families. *Journal of Clinical Oncology.* 2005; 23: 685-693.

[4]: Dispenzieri A., and Kyle R. A. Multiple myeloma: clinical features and indications for therapy. *Best Practice & Research Clinical Haematology*. 2005; 18: 553-568.

[5]: Morgan G. J., Walker B. A., and Davies F. E. The genetic architecture of multiple myeloma. *Nature Reviews Cancer*. 2012; 12: 335-348.

[6]: Kyle R.A., Therneau T. M., Rajkumar S.V., et al. Prevalence of monoclonal gammopathy of undetermined significance. *New England Journal of Medicine.* 2006; 354: 1362-1369.

[7]: Kyle R. A., Therneau T. M., Rajkumar S. V., et al. A long-term study of prognosis in monoclonal gammopathy of undetermined significance. *New England Journal of Medicine.* 2002; 346:564-569.

[8]: Kyle R.A., Remstein E. D., Therneau T. M. et al. Clinical course and prognosis of smoldering (asymptomatic) multiple myeloma. *New England Journal of Meicine.* 2007; 356: 2582-2590.

[9]: Malpas J. S., Bergsagel D. E., Kyle R., Anderson K. Multiple Myeloma: Biology and Management. *Oxford University Press*. 1998; 187-209.

[10]: Rajkumar S.V., Fonseca R., Dewald G.W., Therneau T. M., Lacy M. Q., Kyle R. A. *et al*. Cytogenetic abnormalities correlate with the plasma cell labeling index and extent of bone marrow involvement in myeloma. *Cancer Genetics and Cytogenetics.* 1999; 113: 73-77.

[11]: Zandecki M., Lai J.L., Facon T. Multiple myeloma: almost all patients are cytogenetically abnormal. *British Journal of Haematology.* 1996; 94: 217-227.

[12]: Gonzalez D., van der B.M., Garcia-Sanz R., Fenton J.A., Langerak A.W., Gonzalez M., et al. Immunoglobulin gene rearrangements and the pathogenesis of multiple myeloma. *Blood.* 2007; 110: 3112-3121.

[13]: Bakkus M.H., Heirman C., van Riet I., van Camp B. and Thielemans K. Evidence that multiple myeloma Ig heavy chain VDJ genes contain somatic mutations but show no intraclonal variation. *Blood.* 1992; 80: 2326-2335.

[14]: Bergsagel P.L., Chesi M., Nardini E., et al. Promiscuous translocations into immunoglobulin heavy chain switch regions in multiple myeloma. PNAS USA.1996; 93: 13931-13936

[15]: Bergsagel P.L. and Kuehl W. M. Chromosome translocations in multiple myeloma, *Oncogene,* 2001; 20: 5611-5622.

[16]: Pratt G., Fenton J. A., Proffitt J. A., et al. True spectrum of 14q32 translocations in multiple myeloma. *British Journal of Haematology*. 1998; 103:1209-1210.

[17]: Fonseca R., Bailey R. J., Ahmann G. J., et al. Genomic abnormalities in monoclonal gammopathy of undetermined significance. *Blood.* 2002; 100: 1417-1424.

[18]: Avet-Loiseau H., Facon T., Grosbois B. et al. Oncogenesis of multiple myeloma: 14q32 and 13q chromosomal abnormalities are not randomly distributed, but correlate with natural history, immunological features, and clinical presentation. *Blood.* 2002; 99: 2185-2191.

[19]: Fonseca R., Blood E., Rue M. et al. Clinical and biologic implications of recurrent genomic aberrations in myeloma. *Blood*. 2003; 101: 4569–4575.

[20]: Chng W.J., Glebov O., Bergsagel P.L., Kuehl W.M. Genetic events in the pathogenesis of multiple myeloma. *Best Practice & Research Clinical Haematology.* 2007; 20: 571-596.

[21]: Keats J. J., Reiman T., Maxwell C. A. et al. In multiple myeloma, t(4;14)(p16;q32) is an adverse prognostic factor irrespective of FGFR3 expression. 2003. *Blood*. 101: 1520–1529.

[22]: Chesi M., Nardini E., Lim R. S. C., Smith K. D., Kuehl W. M., and Bergsagel P. L. The t(4;14) translocation in myeloma dysregulates both FGFR3 and a novel gene, MMSET, resulting in IgH/MMSET hybrid transcripts. *Blood*. 1998; 92: 3025–3034.

[23]: Santra M., Zhan F., Tian E., Barlogie B., and Shaughnessy J. Jr. A subset of multiple myeloma harboring the t(4;14)(p16;q32) translocation lacks FGFR3 expression but maintains an IGH/MMSET fusion transcript. *Blood*. 2003; 101: 2374–2376.

[24]: Zhan F., Huang Y., Colla S. et al. The molecular classification of multiple myeloma. *Blood*. 2006; 108: 2020–2028.

[25]: Chesi M., Nardini E., Brents L. A. et al. Frequent translocation t(4;14)(p16.3;q32.3) in multiple myeloma is associated with increased expression and activating mutations of fibroblast growth factor receptor 3. *Nature Genetics.* 1997; 16: 260-264.

[26]: Chesi M., Brents L. A., Ely S. A. et al. Activated fibroblast growth factor receptor 3 is an oncogene that contributes to tumor progression in multiple myeloma. *Blood*. 2001; 97:729-736.

[27]: Martinez-Garcia E., Popovic R., Min D-J., et al. The MMSET histone methyl transferase switches global histone methylation and alters gene expression in t(4;14) multiple myeloma cells. *Blood*. 2011; 117: 211–220.

[28]: Pei H., Zhang L., Luo K. et al. MMSET regulates histone H4K20 methylation and 53BP1 accumulation at DNA damage sites. *Nature*. 2011; 470: 124–128.

[29]: J. Shaughnessy Jr., A. Gabrea, Y. Qi et al. Cyclin D3 at 6p21 is dysregulated by recurrent chromosomal translocations to immunoglobulin loci in multiple myeloma. *Blood*. 2001; 98: 217-223.

[30]: Chesi M., Bergsagel P. L., Brents L. A., Smith C. M., Gerhard D. S., and Kuehl W. M. Dysregulation of cyclin D1 by translocation into an IgH gamma switch region in two multiple myeloma cell lines. *Blood*. 1996; 88: 674–681.

[31]: Avet-Loiseau H., Attal M., Moreau P. et al. Genetic abnormalities and survival in multiple myeloma: the experience of the Intergroupe Francophone du Myélome. *Blood*. 2007; 109: 3489–3495.

[32]: Hurt E. M., Wiestner A., Rosenwald A. et al. Overexpression of c-maf is a frequent oncogenic event in multiple myeloma that promotes proliferation and pathological interactions with bone marrow stroma. *Cancer Cell*. 2004; 5: 191–199.

[33]: Suzuki A., Iida S., Kato-Uranishi M. et al. ARK5 is transcriptionally regulated by the Large-MAF family and mediates IGF-1-induced cell invasion in multiple myeloma: ARK5 as a new molecular determinant of malignant multiple myeloma. *Oncogene*. 2005; 24: 6936-6944.

[34]: Ross F. M., Ibrahim A. H., Vilain-Holmes A. et al. Age has a profound effect on the incidence and significance of chromosome abnormalities in myeloma. *Leukemia*. 2005; 19: 1634–1642.

[35]: Avet-Loiseau H., Malard F., Campion L. et al. Translocation t(14;16) and multiple myeloma: is it really an independent prognostic factor? *Blood*. 2011; 117: 2009–2011.

[36]: Ross F. M., Chiecchio L., Dagrada G. et al. The t(14;20) is a poor prognostic factor in myeloma but is associated with long term stable disease in monoclonal gammopathies of undetermined significance. *Haematologica*. 2010; 95: 1221–1225.

[37]: Dib A., Gabrea A., Glebov O. K., Bergsagel P. L., and Kuehl W. M. Characterization of MYC translocations in multiple myeloma cell lines. *JNCI Monographs.* 2008; 39: 25–31.

[38]: Avet-Loiseau H., Gerson F., Magrangeas F., Minvielle S., Harousseau J.L., and Bataille R. Rearrangements of the c-myc oncogene are present in 15% of primary human multiple myeloma tumors. *Blood*. 2001; 98: 3082–3086.

[39]: Decaux O., Lodé L., Magrangeas F., Charbonnel C., Gouraud W., Jézéquel P., et al. Prediction of survival in multiple myeloma based on gene expression profiles reveals cell cycle and chromosomal instability signatures in high-risk patients and hyperdiploid signatures in low-risk patients: a study of the Intergroupe Francophone du Myélome. *Journal of Clinical Oncology.* 2008; 26: 4798-4805.

[40]: Greipp P. R., SanMiguel J., Durie B. G. et al. International staging system for multiple myeloma. *Journal of Clinical Oncology.* 2205; 23: 3412–3420.

[41]: Gabrea A., Martelli M. L., Qi Y. et al. Secondary genomic rearrangements involving immunoglobulin or MYC loci show similar prevalences in hyperdiploid and nonhyperdiploid myeloma tumors. *Genes Chromosomes and Cancer*. 2008; 47: 573–590.

[42]: Smadja N. V., Leroux D., Soulier J. et al. Further cytogenetic characterization of multiple myeloma confirms that 14q32 translocations are a very rare event in hyperdiploid cases. *Genes Chromosomes Cancer*. 2003; 38: 234-239.

[43]: Smadja N. V., Bastard C., Brigaudeau C., Leroux D., and Fruchart C. Hypodiploidy is a major prognostic factor in multiple myeloma. *Blood*. 2001; 98: 2229–2238.

[44]: Fonseca R., Bes-Marun C. S., Picken E. B. et al. The recurrent IgH translocations are highly associated with nonhyperdiploid variant multiple myeloma. *Blood*. 2003; 102: 2562-2567.

[45]: Avet-Loiseau H., Daviet A., Brigaudeau C. et al. Cytogenetic, interphase, and multicolor fluorescence in situ hybridization analyses in primary plasma cell leukemia: a study of 40 patients at diagnosis, on behalf of the Intergroupe Francophone du Myélome and the Groupe Francais de Cytogenetique Hematologique. *Blood*. 2001; 97: 822-825.

[46]: Onodera N., McCabe N. R., and Rubin C.M. Formation of a hyperdiploid karyotype in childhood acute lymphoblastic leukemia. *Blood*. 1992: 80: 203–208.

[47]: Chng W. J., Kumar S., Wier S. et al. Molecular dissection of hyperdiploid multiple myeloma by gene expression profiling. *Cancer Research.* 2007; 67: 2982–2989.

[48]: Avet-Loiseau H., Facon T., Daviet A. et al. 14q32 translocations and monosomy 13 observed in monoclonal gammopathy of undetermined significance delineate a multistep process for the oncogenesis of multiple myeloma. Intergroupe Francophone du Myélome. *Cancer Research.* 1999; 59: 4546-4550.

[49]: Facon T., Avet-Loiseau H., Guillerm G. et al. Chromosome 13 abnormalities identified by FISH analysis and serum beta2-microglobulin produce a powerful myeloma staging system for patients receiving high-dose therapy. *Blood*. 2001; 97:1566-1571.

[50]: Fonseca R., Harrington D., Oken M. M. et al. Biological and prognostic significance of interphase fluorescence in situ hybridization detection of chromosome 13 abnormalities (delta13) in multiple myeloma: an eastern cooperative oncology group study. *Cancer Research.* 2002; 62:715-720.

[51]: Avet-Loiseau H., Daviet A., Sauner S., Bataille R. Chromosome 13 abnormalities in multiple myeloma are mostly monosomy 13. *British Journal of Haematology.* 2000; 111: 1116-1117.

[52]: Fonseca R., Oken M. M., Harrington D. et al. Deletions of chromosome 13 in multiple myeloma identified by interphase FISH usually denote large deletions of the q arm or monosomy. *Leukemia* 2001; 15: 981-986.

[53]: Walker B. A., Leone P. E., Chiecchio L. et al. A compendium of myeloma-associated chromosomal copy number abnormalities and their prognostic value. *Blood*. 2010; 116: e56–e65.

[54]: Fonseca R., Bergsagel P. L., Drach J. et al. International Myeloma Working Group molecular classification of multiple myeloma: spotlight review. *Leukemia*. 2009; 23: 2210– 2221.

[55]: Tricot G., Barlogie B., Jagannath S. et al. Poor prognosis in multiple myeloma is associated only with partial or complete deletions of chromosome 13 or abnormalities involving 11q and not with other karyotype abnormalities. *Blood*. 1995; 86: 4250–4256.

[56]: Pérez-Simón J. A., García-Sanz R., Tabernero M. D. et al. Prognostic value of numerical chromosome aberrations in multiple myeloma: a FISH analysis of 15 different chromosomes. *Blood*. 1998; 91: 3366–3371.

[57]: Chng W. J., Santana-Dàvila R., Wier S. A. et al. Prognostic factors for hyperdiploid-myeloma: effects of chromosome 13 deletions and IgH translocations. *Leukemia*. 2006; 20: 807–813.

[58]: Boyd K. D., Ross F. M., Walker B. A. et al. Mapping of chromosome 1p deletions in myeloma identifies FAM46C at 1p12 and CDKN2C at 1p32.3 as being genes in regions associated with adverse survival. *Clinical Cancer Research.* 2011; 17: 7776–7784.

[59]: Chang H., Jiang A., Qi C., Y. Trieu, C. Chen, and D. Reece. Impact of genomic aberrations including chromosome 1 abnormalities on the outcome of patients with relapsed or refractory multiple myeloma treated with lenalidomide and dexamethasone. *Leukemia and Lymphoma*. 2010; 51: 2084–2091.

[60]: Chapman M. A., Lawrence M. S., Keats J. J. et al. Initial genome sequencing and analysis of multiple myeloma. *Nature*. 2011; 471: 467–472.

[61]: Chang H., Qi X., Jiang A., Xu W., Young T. and Reece D. 1p21 deletions are strongly associated with 1q21 gains and are an independent adverse prognostic factor for the outcome of high-dose chemotherapy in patients with multiple myeloma. *Bone Marrow Transplantation.* 2010; 45: 117–121.

[62]: Leone P. E., Walker B. A., Jenner M. W. et al. Deletions of CDKN2C in multiple myeloma: biological and clinical implications. *Clinical Cancer Research.* 2008; 14: 6033–6041.

[63]: Tiedemann R. E., Gonzalez-Paz N., Kyle R. A. et al. Genetic aberrations and survival in plasma cell leukemia. *Leukemia*. 2008; 22: 1044–1052.

[64]: Lodé L., Eveillard M., Trichet V. et al. Mutations in TP53 are exclusively associated with del(17p) in multiple myeloma. *Haematologica*. 2010; 95: 1973–1976.

[65]: Drach J., Ackermann J., Fritz E. et al. Presence of a p53 gene deletion in patients with multiple myeloma predicts for short survival after conventional-dose chemotherapy. *Blood*. 1998; 92: 802–809.

[66]: Jenner M. W., Leone P. E., Walker B. A. et al. Gene mapping and expression analysis of 16q loss of heterozygosity identifies WWOX and CYLD as being important in determining clinical outcome in multiple myeloma *Blood*. 2007; 110: 3291– 3300.

[67]: Annunziata C. M., Davis R. E., Demchenko Y. et al. Frequent engagement of the classical and alternative NF-*κ*B pathways by diverse genetic abnormalities in multiple myeloma. *Cancer Cell*. 2007; 12: 115-130.

[68]: Keats J. J., Fonseca R., Chesi M. et al. Promiscuous mutations activate the noncanonical NF-*κ*B pathway in multiple myeloma. *Cancer Cell*. 2007; 12: 131–144.

[69]: Sutlu T., Alici E., Jansson M. et al. The prognostic significance of 8p21 deletion in multiple myeloma. *British Journal of Haematology*. 2009; 144: 266–268.

[70]: Gmidéne A., Saad A., and Avet-LoiseauH. 8p21.3 deletion suggesting a probable role of TRAIL-R1 and TRAIL-R2 as candidate tumor suppressor genes in the pathogenesis of multiple myeloma. *Medical Oncology*. 2013; 30: 489.

[71]: Gazitt Y. TRAIL is a potent inducer of apoptosis in myeloma cells derived from multiple myeloma patients and is not cytotoxic to hematopoietic stem cells. *Leukemia*. 1999; 13: 1817–1824.

[72]: Fonseca R., Wier S. A., Chng W. J. et al. Prognostic value of chromosome 1q21 gain by fluorescent in situ hybridization and increase CKS1B expression in myeloma. *Leukemia*. 2006; 20: 2034-2040.

[73]: Hanamura I., Stewart J. P., Huang Y., et al. Frequent gain of chromosome band 1q21 in plasma-cell dyscrasias detected by fluorescence in situ hybridization: incidence increases from MGUS to relapsed myeloma and is related to prognosis and disease progression following tandem stem-cell transplantation. *Blood.* 2006; 108: 1724-1732.

[74]: Cremer F. W., Bila J., Buck I., et al. Delineation of distinct subgroups of multiple myeloma and a model for clonal evolution based on interphase cytogenetics. *Genes Chromosomes Cancer*. 2005; 44: 194-203.

[75]: Nemec P., Zemanova Z., Greslikova H., Michalova K., Filkova H., Tajtlova J., *et al.* Gain of 1q21 is an unfavorable genetic prognostic factor for multiple myeloma patients treated with high-dose chemotherapy. *Biology of Blood and Marrow Transplantation.* 2010; 4: 548-554.

[76]: An G., Xu Y., Shi L., Shizhen Z., Deng S., Xie Z., et al. Chromosome 1q21 gains confer inferior outcomes in multiple myeloma treated with bortezomib but copy number variation and percentage of plasma cells involved have no additional prognostic value. *Haematologica*. 2014; 2: 353-359.

[77]: Carrasco D. R., Tonon G., Huang Y., Zhang Y., Sinha R., Feng B., Stewart J. P., Zhan F., Khatry D., Protopopova M., Protopopov A., Sukhdeo K., Hanamura I., Stephens O., Barlogie B., Anderson K. C., Chin L., Shaughnessy J. D. Jr., Brennan C., Depinho R. A. High-resolution genomic profiles defines distinct clinico-pathogenetic subgroups of multiple myeloma patients. *Cancer Cell*. 2006; 4: 313–325.

[78]: Fabris S., Ronchetti D., Agnelli L., Baldini L., et al. Transcriptional features of multiple myeloma patients with chromosome 1q gain. *Leukemia.* 2007; 21: 1113-1116.

[79]: Agnelli L., Mosca L., Fabris S., Lionetti M., et al. A SNP microarray and FISH-based procedure to detect allelic imbalances in multiple myeloma: an integrated genomics approach reveals a wide gene dosage effect. *Genes Chromosomes Cancer.* 2009; 48: 603-614.

[80]: Shaugnessy J.D. Jr., Qu P., Usmani S., Heuck C. J. et al. Pharmacogenomics of bortezomib test-dosing identifies hyperexpression of proteasome genes, especially PSMD4, as novel high-risk feature in myeloma treated with Total Therapy 3. *Blood*. 2011; 118: 3512-3524.

[81]: Neben K., Lokhorst H. M., Jauch A., Bertsch U., et al. Administration of bortezomib before and after autologous stem cell transplantation improves outcome in multiple myeloma patients with deletion 17p. *Blood.* 2012; 119: 940-948.

[82]: Liu H., Tamashiro S., Baritaki S., et al. TRAF6 activation in multiple myeloma: a potential therapeutic target. *Clin. Lymph. Myeloma and Leukemia*. 2012; 12: 155–163.

[83]: Hideshima T, Chauhan D, Richardson P, et al. NF-kappa B as a therapeutic target in multiple myeloma. J Biol Chem. 2002;277:16639-16647.

[84]: Raje N, Hideshima T, Anderson KC. Therapeutic use of immunomodulatory drugs in the treatment of multiple myeloma. *Expert Review of Anticancer Therapy.* 2006; 6: 1239-1247.

[85]: Chng W. J., Gonzalez-Paz N., Price-Troska T. et al. Clinical and biological significance of RAS mutations in multiple myeloma. *Leukemia*. 2008; 12: 2280-2284.

[86]: Bezieau S., Devilder M. C., vet-Loiseau H. et al. High incidence of N and K-Ras activating mutations in multiple myeloma and primary plasma cell leukemia at diagnosis. *Human Mutation.* 2001; 18: 212-224.

[87]: Rasmussen T., Kuehl M., Lodahl M., Johnsen H. E. and Dahl I. M. S. Possible roles for activating RAS mutations in the MGUS to MM transition and in the intramedullary to extramedullary transition in some plasma cell tumors. *Blood*. 2005; 105: 317–323.

[88]: Bharti A. C., Shishodia S., Reuben J. M. et al. Nuclear factor-κB and STAT3 are constitutively active in CD138+ cells derived from multiple myeloma patients, and suppression of these transcription factors leads to apoptosis. *Blood*. 2004; 103: 3175–3184.

[89]: Catlett-Falcone R., Landowski T. H., Oshiro M. M. et al. Constitutive activation of Stat3 signaling confers resistance to apoptosis in human U266 myeloma cells. *Immunity*. 1999; 10: 105–115.

[90]: Kawano M., Hirano T., Matsuda T. et al. Autocrine generation and requirement of BSF-2/IL-6 for human multiple myelomas. *Nature*. 1988; 332: 83–85.

[91]: Catlett-Falcone R., Landowski T. H. , Oshiro M. M., et al. Constitutive activation of Stat3 signaling confers resistance to apoptosis in human U266 myeloma cells. *Immunity.* 1999;10: 105–115.

[92]: Chatterjee M., Stuhmer T., Herrmann P. et al. Combined disruption of both the MEK/ERK and the IL-6R/STAT3 pathways is required to induce apoptosis of multiple myeloma cells in the presence of bone marrow stromal cells. *Blood.* 2004; 104: 3712-3721.

[93]: Aronson L., Davenport E., Giuntoli S. et al. Autophagy is a key myeloma survival pathway that can be manipulated therapeutically to enhance apoptosis. *ASH Annual Meeting Abstracts*. 2010; 116: 4083.

[94]: F. E. Davies. Biological characterization of multiple myeloma. *EHA Oncoletter*, 17th Congress of European Hematology Association 2012; 6: 213-220.

[95]: Mitsiades C. S., Davies F. E., Laubach J. P., Joshua D., San Miguel J., Anderson K. C., et al. Future directions of next-generation novel therapies, combination approaches, and the development of personalized medicine in myeloma. *Journal of Clinical Oncology.* 2011; 29: 1916-23.

[96]: Bergsagel P. L., Kuehl W. M., Zhan F., Sawyer J., Barlogie B. and Shaughnessy J. Cyclin D dysregulation: an early and unifying pathogenic event in multiple myeloma. *Blood*. 2005;106:296-303.

[97]: Sawyer J. R., Tian E., Heuck C. J., Johann D. J. et al. Evidence of an epigenetic origin for high-risk 1q21 copy number aberrations in multiple myeloma. *Blood*. 2015; 125: 3756-3759.

[98]: Kim D., Pertea G., Trapnell C., Pimentel H., Kelley R., Salzberg S. L. TopHat2: accurate alignment of transcriptomes in the presence of insertions, deletions and gene fusions. *Genome Biology.* 2013; 14: 1-13.

[99]: Love M.I., Huber W., Anders S. Moderated estimation of fold change and dispersion for RNA-seq data with DESeq2. *Genome Biology.* 2014; 15: 1-21.

[100]: Shen S., Park J.W., Lu Z.X., Lin L., Henry M.D., Wu Y.N., Zhou Q., Xing Y. rMATS: robust and flexible detection of differential alternative splicing from replicate RNA-Seq data. *Proc Natl Acad Sci U S A.* 2014; 23; 111: 5593-5601.

[101]: Fenech M. Cytokinesis-block micronucleus cytome assay. *Nature protocols.* 2007; 2: 1084-1104.

[102]: Ma C.X., Cai S., Li S., Ryan C.E., Guo Z, Schaiff W.T., Lin L., Hoog J., Goiffon R.J., Prat A., Aft R. L., Ellis M.J., Piwnica-Worms H. Targeting Chk1 in p53-deficient triple-negative breast cancer is therapeutically beneficial in human-in-mouse tumor models. *The Journal of Clinical Investigation.* 2012; 122: 151-1552.

[103]: Beroukhim R., Getz G., Nghiemphu L., Barretina J., Hsueh T., Linhart D. et al. Assessing the significance of chromosomal aberrations in cancer: methodology and application to glioma. *Proc Natl Acad Sci U S A.* 2007; 104: 20007-20012.

[104]: Zhang B., Gojo I., and Fenton R. G. Myeloid cell factor-1 is a critical survival factor for multiple myeloma. *Blood*. 2002; 99: 1885-1893.

[105]: Dutertre M., Lambert S., Carreira A., Amor-Guéret M., Vagner S. DNA damage: RNA-binding proteins protect from near and far. *Trends in Biochemical Sciences.* 2014; 39: 141-149.

[106]: Guan D., Altan-Bonnet N., Parrott A. M., Arrigo C. J., Li Q., Khaleduzzaman M., Li H., Lee C. G., Pe'ery T., Mathews M. B. Nuclear Factor 45 (NF45) Is a Regulatory Subunit of Complexes with NF90/110 Involved in Mitotic Control. *Molecular and Cellular Biology.* 2008; 28: 4629–4641.

[107]: Shamanna R.A., Hoque1 M., Pe'ery T. and Mathews M. B. Induction of p53, p21 and apoptosis by silencing the NF90/NF45 complex in human papilloma virus-transformed cervical carcinoma cells. *Oncogene.* 2013; 32:5176–5185.

[108]: Grzasko N., Hus M., Pluta A., Jurczyszyn A., Walter-Croneck A., Morawska M. et al. Additional genetic abnormalities significantly worsen poor prognosis associated with

1q21 amplification in multiple myeloma patients. *Hematological Oncology.* 2013; 31: 41-48.

[109]: Mani M., Carrasco D. E., Zhang Y., Takada K., Gatt M. E. et al. BCL9 promotes tumor progression by conferring enhanced proliferative, metastatic, and angiogenic properties to cancer cells. *Cancer research*. 2009; 69: 7577-7586.

[110]: P. Sonneveld. Gain of 1q21 in multiple myeloma: from bad to worse? *Blood*. 108: 1426-27.

[111]: Shaughnessy J. Amplification and overexpression of CKS1B at chromosome band 1q21 is associated with reduced levels of $p27^{Kip1}$ and an aggressive clinical course in multiple myeloma. *Hematology*. 2005; 10: 117-126.

[112]: Zhan F., Colla S., Wu X., Chen B., Stewart J. P., Kuehl W. M., Barlogie B. and Shaughnessy D. Jr. *CKS1B*, overexpressed in aggressive disease, regulates multiple myeloma growth and survival through SKP2- and $p27^{Kip1}$-dependent and -independent mechanisms. *Blood.* 2007; 109: 4995-5001

[113]: Treon S. P., Maimonis P., Bua D., Young G., Raje N., Mollick J. et al. Elevated soluble MUC1 levels and decreased anti-MUC1 antibody levels in patients with multiple myeloma. *Blood.* 2000; 96: 3147-3153.

[114]: Takahashi T., Makiguchi Y., Hinoda Y. et al. Expression of Muc1 on myeloma cells and induction of HLA unrestricted CTL against Muc1 from a multiple myeloma patient. *Journal of Immunology.* 1994; 153: 2102-2109

[115]: Yin L., Kufe T., Avigan D., and Kufe D. Targeting MUC1-C is synergistic with bortezomib in downregulating TIGAR and inducing ROS-mediated myeloma cell death. *Blood.* 2014; 123: 2997-3006.

[116]: Kocher O., Comella N., Gilchrist A., Pal R., Tognazzi K., Brown L. F., Knoll J. H. PDZK1, a novel PDZ domain-containing protein up-regulated in carcinomas and mapped to chromosome 1q21, interacts with cMOAT (MRP2), the multidrug resistance-associated protein. Laboratory Investigation.1999;79: 1161–1170.

[117]: Inoue J., Otsuki T., Hirasawa A., Imoto I., Matsuo Y., Shimizu S., Taniwaki M, and Inazawa J. Overexpression of *PDZK1* within the 1q12-q22 Amplicon Is Likely To Be Associated with Drug-Resistance Phenotype in Multiple Myeloma. *American Journal of Pathology*. 2004; 165: 71-81

[118]: Shamanna A. R., Hoque M., Lewis-Antes A., Azzam I. E., Lagunoff D., Pe'ery T., and Mathews M. B. The NF90/NF45 Complex Participates in DNA Break Repair via Nonhomologous End Joining. *Molecular and Cellular Biology.* 2011; 31: 4832–4843.

[119]: Zhao G., Shi L., Qiu D., Hu H., Kao P. N. NF45/ILF2 tissue expression, promoter analysis, and interleukin-2 transactivating function. *Experimental Cell Research.* 2004; 305: 312– 323.

[120]: Ting N. S., Kao P. N., Chan D. W., Lintott L. G., Lees-Miller S.P. DNA dependent protein kinase interacts with antigen receptor response element binding proteins NF90 and NF45. 1998; *The Journal of Biological Chemistry.* 273: 2136–2145.

[121]: Sakamoto S., Aoki K., Higuchi T., Todaka H., Morisawa K., Tamaki N. et al. The NF90-NF45 complex functions as a negative regulator in the microRNA processing pathway. *Molecular and Cellular Biology.* 2009; 29:3754–3769.

[122]: Merrill M. K., Gromeier M. The double-stranded RNA binding protein 76: NF45 heterodimer inhibits translation initiation at the rhino virus type 2 internal ribosome entry site. *Journal of Virology*. 2006; 80: 6936–6942.

[123]: Stricker R. L., Behrens S. E., Mundt E. Nuclear factor NF45 interacts with viral proteins of infectious bursal disease virus and inhibits viral replication. *Journal of Virology.* 2010; 84: 10592–10605.

[124]: Aaboe M., Marcussen N., Jensen K. M., Thykjaer T., Dyrskjot L., Orntoft T. F. Gene expression profiling of noninvasive primary urothelial tumours using microarrays. British Journal of Cancer. 2205; 93:1182–1190.

[125]: Vumbaca F., Phoenix K. N., Rodriguez-Pinto D., Han D. K., Claffey K. P. Double-stranded RNA-binding protein regulates vascular endothelial growth factor mRNA

stability, translation, and breast cancer angiogenesis. *Molecular and Cellular Biology.* 2008; 28:772–783.

[126]: Hu Q., Lu Y. Y., Noh H., Hong S., Dong Z., Ding H. F., Su S. B. and Huang S. Interleukin enhancer-binding factor 3 promotes breast tumor progression by regulating sustained urokinase-type plasminogen activator expression. *Oncogene.* 2013; 32: 3933–3943.

[127]: Ni T., Mao G., Xue Q., Liu Y., Chen B. et al. Upregulated expression of ILF2 in non-small cell lung cancer is associated with tumor cell proliferation and poor prognosis. *Journal of Molecular Histology.* 2015; 46: 325–335.

[128]: Huang Q., He X., Qiu X., Liu X., Sun G., Guo J., Ding Z. et al. Expression of NF45 correlates with malignant grade in gliomas and plays a pivotal role in tumor growth. Tumor Biology. 2014; 35: 10149‑10157.

[129]: Shkreta L. and Chabot B. The RNA Splicing Response to DNA Damage. *Biomolecules.* 2015; 5: 2935-2977.

[130]: Montecucco A. and Biamonti G. Pre-mRNA processing factors meet the DNA damage response. *Frontiers in Genetics.* 2013; 4: 1-14.

[131]: Chatterjee M., Rancso C., Stühmer T., Eckstein N., Andrulis M. et al. The Y-box binding protein YB-1 is associated with progressive disease and mediates survival and drug resistance in multiple myeloma. *Blood.* 2008; 111: 3714-3722.

[132]: Lee Y. Y., McKinney K. Q., Ghosh S., Iannitti D. A., Martinie J. B. et al. Subcellular Tissue Proteomics of Hepatocellular Carcinoma for Molecular Signature Discovery. *Journal of Proteome Research.* 2011; 10: 5070–5083.

[133]: Hu Q., Lu Y. Y., Noh H., Hong S., Dong Z. Interleukin enhancer-binding factor 3 promotes breast tumor progression by regulating sustained urokinase-type plasminogen activator expression. *Oncogene.* 2013; 32: 3933–3943.

[134]: Chung F. H., Lee H. H. C., Lee H. C. ToP: A Trend-of-Disease-Progression Procedure Works Well for Identifying Cancer Genes from Multi-State Cohort Gene Expression Data for Human Colorectal Cancer. *Plos One.* 2013; 8: 1-13.

[135]: The International Myeloma Working Group: Criteria for the classification of monoclonal gammopathies, multiple myeloma and related disorders: a report of the International Myeloma Working Group. *British Journal of Haematology.* 2003; 121: 749–757.

[136]: Durie B. G. M. , Harousseau J. L., Miguel J. S., Blade´ J., Barlogie B., Anderson K. et al. International uniform response criteria for multiple myeloma. *Leukemia.* 2006; 20: 1467–1473.

[137]: Bergsagel P. L and Kuehl W. M. Molecular pathogenesis and a consequent classification of Multiple Myeloma. *Journal of Clinical Oncology.* 2005. 23; 6333-6338.